Investigation of Dempster Highway Sinkholes

km 82 and Two Moose Lake

Northern Climate ExChange
YUKON RESEARCH CENTRE • Yukon College

Transports Canada Transport Canada

This publication may be obtained online at yukoncollege.yk.ca/research.

THIS PUBLICATION MAY BE OBTAINED FROM:
Yukon Research Centre, Yukon College
520 College Drive, PO Box 2799
Whitehorse, Yukon Y1A 5K4
(867) 668-8895 or 1 (800) 661-0504

Recommended citation:
Calmels, F., Roy, L.P., Laurent, C. and Horton, B. 2017. Investigation of Dempster Highway Sinkholes: km 82 and Two Moose Lake. Yukon Research Centre, Yukon College, 66 p.

Photo Credit: *Fabrice Calmels, Northern Climate ExChange, Yukon Research Centre, Yukon College*

PROJECT TEAM

Authors

Fabrice Calmels	Northern Climate ExChange, Yukon Research Centre, Yukon College
Louis Philippe Roy	Northern Climate ExChange, Yukon Research Centre, Yukon College
Cyrielle Laurent	Northern Climate ExChange, Yukon Research Centre, Yukon College
Brian Horton	Northern Climate ExChange, Yukon Research Centre, Yukon College

Disclaimer

TABLE OF CONTENTS

1. INTRODUCTION

This report presents the results of a project that aims to understand and, if possible, recommend actions to remediate the issues caused by the formation of sinkholes at km 82 and km 102-103 of the Dempster Highway. At km 82, this has resulted in sudden collapse of the right-hand side driving surface of the highway. Major sinkholes have been repaired at this location on at least two occasions (June 2014 and Aug 2014) and the culvert at the site was replaced in October 2014. Undated photos suggest earlier sinkholes have formed at this location (SRK Consulting, 2014). Subsidence was also repaired in August 2015. At km 102-103, there has been general subsidence and sinkhole formation along the left-hand side of the road. Subsidence between km 102 and 103 has been regularly repaired as part of routine highway maintenance and is therefore not documented. At this site, Two-Moose Lake is now encroaching on the road embankment.

This project included various activities. The first step consisted of a preliminary assessment and literature review, where data and report from previous surveys and studies pertaining to the study area and its surroundings were reviewed. Additional information such as articles, air photos, satellite imagery, geological and surficial geological maps have been reviewed to gain insight about the geomorphologic and surficial geologic conditions of the area.

The preliminary assessment was followed by a field assessment, from July 20th to 30th 2016, that focused on the foot of the embankment and the field area adjacent to the embankment at km 82 and between km 102 and 103. Work on both sides of the road included a combination of drilling, electrical resistivity tomography (ERT), and installation of ground temperature monitoring instruments. Core samples collected during drilling were kept frozen and returned to the Northern Climate ExChange (NCE) lab in Whitehorse for further analyses.

This report presents the results of the field, laboratory, and desktop assessment. Subsequent sections include the following:

- Description of geologic and geomorphologic context including discussion of surficial geology, glacial history and permafrost geomorphology;
- Review of methodology, summarizing the techniques used for the surveys and their underlying principles;
- Review of findings from previous surveys performed at the study sites;
- Presentation and discussion of the newly collected data; hypotheses of the origin and processes leading to sinkholes are presented and supporting evidence is discussed;

- Conclusions summarizing the findings and discussing the possible next steps.

The present work is only intended to determine the nature of the issues at km 82 and between km 102-103. Depending on the nature of the issue, further investigations may be required. While suggestions for remediation actions are provided, it remains HPW's prerogative to determine the action to take to deal with the issue.

2. BIOPHYSICAL CONTEXT

This section, while not an exhaustive review, presents key knowledge about the biophysical setting of the km 82/km 103 region that is required to place the sinkhole processes in their context. Three figures provide the geomorphologic context: Figure 2.1 shows the surficial geology and glacial limit maps for the studied section of the Dempster Highway. Figure 2.2 shows the surficial geology at site-scale for km 82 and km 103. Figure 2.3 shows the glacial limits at same scale for both sites.

The study sites are located in the Ogilvie Mountains, on the Blackstone uplands (km 74 – 160), where the road the road follows valley floors. Surficial materials in the area consist mostly of glacial till, colluvium, and outwash deposits (Figure 2.1). Both studied sites are located north of the last glacial maximum limit (Beierle, 2002). The km 82 site is located of the flank of a west facing hill slope, where the road crosses morainal (till) and colluvial deposits (Figure 2.2). The km 103 site is located on the valley floor (Figure 2.2). A gravel pit located at km 123 indicates the surficial materials are mostly glaciofluvial outwash, covered by a veneer of silt. The site has well developed networks of ice-wedge polygons. These are expressed at the ground surface by slight depressions in the moss and lichen surface vegetation (Burn et al., 2015). In the area, bedrock consists of Paleozoic metasedimentary, ultramafic and sedimentary rocks and is intruded by Cretaceous porphyritic syenite (Green, 1972).

The climate of the region is continental sub-Arctic with long cold winters, short mild summers and relatively low precipitation. Lacelle et al (2007) reports that mean annual air temperatures recorded at the Mayo (504 m a.s.l.) and Keno (1472 m a.s.l.) meteorological station, located approximately 70 km southeast of the study site, are −3.6 °C and −5.1 °C, respectively (Environment Canada, 2004). There are orographic effects inducing topographically controlled temperature inversions in winter, while in summer, temperatures may be ∼5 °C cooler in the highlands (Burn, 1994). These effects also enhance precipitation at higher elevations, as illustrated by the data from Mayo (318 $mm \cdot yr^{-1}$) and Keno (590 $mm \cdot yr^{-1}$).

2.1 Permafrost

The Blackstone uplands are located in the continuous permafrost zone (Heginbottom et al., 1995). Subsurface conditions at km 82 are known from two boreholes drilled down to 7.3 and 13.7 m. These boreholes were drilled in 2014 and 2015, respectively. The boreholes, located 40 m apart, were drilled in proximity of the road embankment on the right hand side, upslope of the highway. At these locations permafrost is significantly disturbed as the road embankment intercepts drainage and favours snow accumulation. HPW reports that this is also a location where snow is piled during winter plowing operations. Borehole logs show coarse material

ranging from silty sand with gravel to silty gravel with sand. Active layers ranged from 6 to 10 m; ground temperature recorded in the second borehole were quite warm, close to thawing at 0°C at the maximal depth of 13.7 m. No ground ice was cored in either borehole.

Subsurface conditions at km 102-103 can be inferred from previous surveys done at the valley floor in the vicinity (km 116 and 124). At km 116, a retrogressive thaw slump has exposed buried massive ice at 2 m depth, and propagating to an unknow depth. At km 124, boreholes were drilled under the road embankment, at its toe, and in the field in 2013. Previous work showed low near-surface annual mean ground temperatures (< -4.0 °C) in the area. However, unfrozen ground and free water were encountered at depth in all drill holes at this site. At the field site, foliated massive ice, interpreted as wedge ice, was recovered in the silts overlying the gravel, and a 0.35-m layer of pool ice was found within the permafrost. The silts were ice rich; the two tested samples had excess ice contents of 49 and 69 %. The underlying outwash gravels included a range of clast sizes including boulders. The boulders prevented deeper drilling. Permafrost has degraded completely beneath the toe of the embankment, while the base of permafrost is at about 7 m depth at both field and centerline sites. The thin layer of permafrost is attributable to heat transfer in groundwater flowing through the glacial outwash at the site. Permafrost at the toe cannot be sustained due to insulation and runoff effects of snow accumulation at the edge of the road from plowing and capture of blown snow in willows and alder bushes. At the centerline within the embankment, permafrost is sustained; its temperature just below the active layer is comparable with the field site (-2.4 °C).

2.2 Glacial history

The study sites are in an area that has been glaciated numerous times by the Cordilleran Ice Sheet and by local mountain glaciers (Figures 2.1 and 2.3). Bostock (1966) identified a series of four advances and retreats of Cordilleran continental glaciers termed the Nansen, Klaza, Reid and McConnell glaciations, from the oldest to the youngest. Each glaciation was less extensive than the previous one. The extent and age of the Nansen and Klaza glaciations are poorly defined across the central Yukon Territory; while the extent of the younger Reid and McConnell glaciations are clearly defined by terminal moraine systems (Froese and Zazula, 2003).

Glaciations have left a variable imprint on the landscape. A central portion of the highway, km 116 to 495, passes through terrain that was not glaciated at all by either the Cordilleran or Laurentide ice sheets. As a result, some sections of the route are dominated by colluvial sediments, or weathered bedrock. In contrast, southern parts of the route, between about km 75 and km 116 km (Figure 1), experienced valley glaciation during the Wisconsinan Glacial period (110,000 –11,700ka), while north and east of km 495 Peel Plateau and the plains of NWT were covered by the Laurentide ice sheet (Burn et al., 2015).

2.3 Significant ground ice

Here we describe the types of ground ice that have been previously observed in the region and which are more likely to be involved in sinkhole processes at the study sites.

2.3.1 Buried Ice

Buried glacier ice has been exposed and described in moraine sediments at km 116 near Chapman Lake (Lacelle *et al*., 2007). The massive ground-ice body was exposed following a retrogressive thaw slump on a hillside cut near the highway. The age of the glacier ice in this location is not known, but as mentioned above, the Blackstone uplands were likely glaciated on numerous occasions during the Pleistocene but prior to the Cordilleran glaciation.

The exposed section was located a northeast facing hillslope. The thaw slump had low gradient slump floor and a near vertical 4-m-high headwall. Two units were visible in the exposed face. Unit 1 consisted of a relatively clean massive ground ice, $\geq$2 m thick, with a few striated clast layers suspended in it. On the north side of the exposure, alternating near-vertical layers of debris-rich and clear ice were found. Unit 2 overlaid Unit 1 and consisted of an icy diamicton at least 2 m thick with a reticulate ice structure near its lower contact that graded upward to a parallel-layered lenticular pattern at the active layer boundary. The contact between the massive ice and the overlying icy diamicton was sharp, suggesting an erosional surface or a thaw unconformity. The contact between the massive ground ice and underlying sediments was covered by slumped debris and could not be observed.

2.3.2 Ice wedges

Patches of ice-wedge polygons are present in the studied area, especially in the valley floor. They were not observed in the proximity of the site at km 82. However, they are visible at km 103, in vicinity of Two Moose Lake. These polygons characteristically have slight depressions above the wedges, and lack the raised rims formed by actively growing ice wedges. At some locations, they are degrading and their troughs are filled with water. They are most commonly seen at tundra sites. The ice wedges are comprised of massive ice, as observed at km 124 (Idrees *et al*., 2015).

2.3.3 Segregated ice

Throughout the study area, segregated ice is likely to be found at the uppermost layers of permafrost where there are unconsolidated, fine-grained sediments. It was not observed in the boreholes at km 82, but was observed in the valley floor in the silt veneer overlying the coarse

morainal or outwash deposits. This ground ice can be syngenetic, developing near the top of permafrost and remain there if the permafrost table rises because of sedimentation and aggradation of the surface, or the rise of the permafrost table in response to periods of colder climate (e.g., French and Shur, 2010). The ice-rich zone has been called the transient layer of permafrost, and is common in frost-susceptible soils. Because it is constrained mostly to the uppermost meters of permafrost and may be much more diffuse downward, it is unlikely to be the cause of the recurring formation of sinkholes.

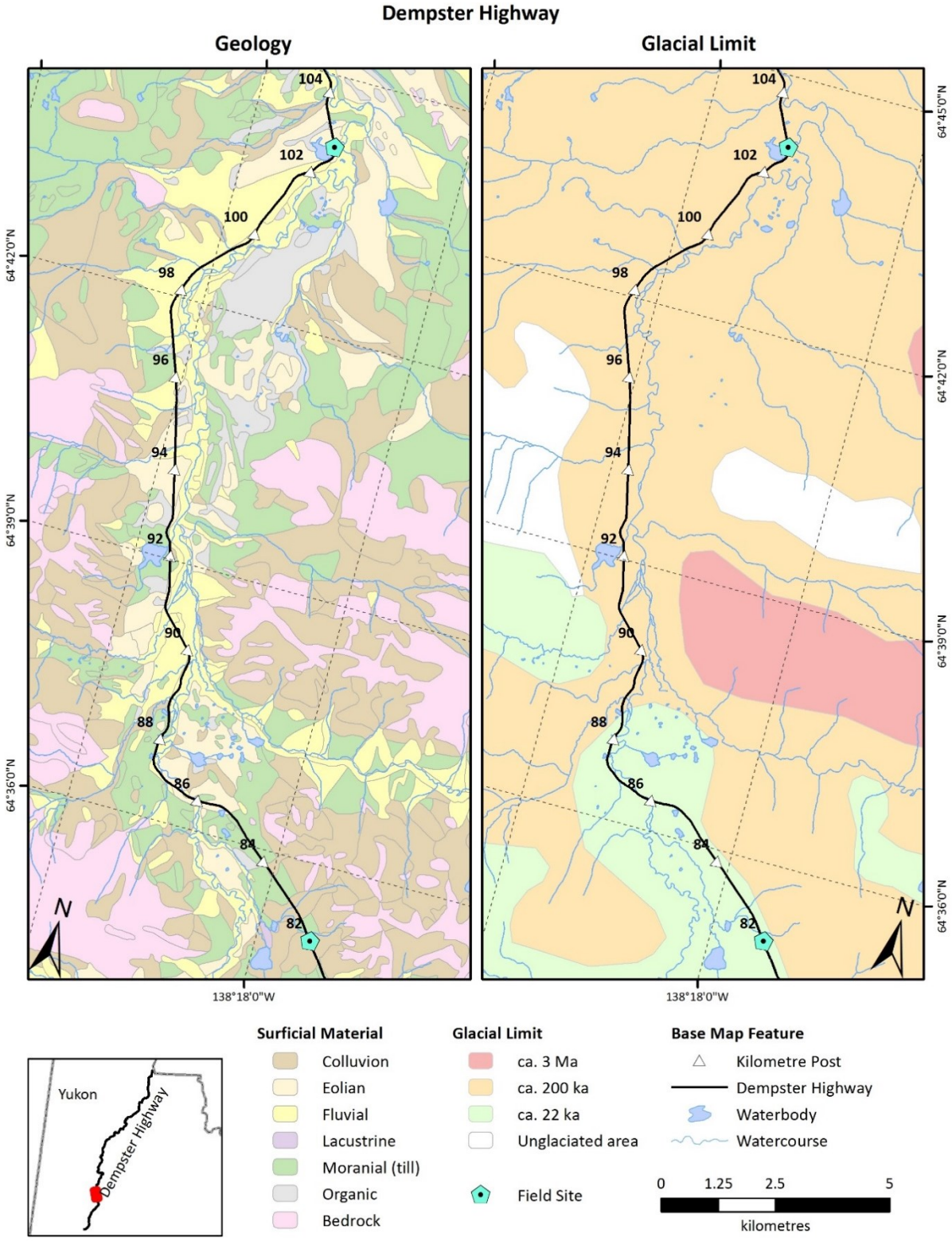

Figure 2.1. Surficial geology and glacial limits in studied area (≈km82 to km104).

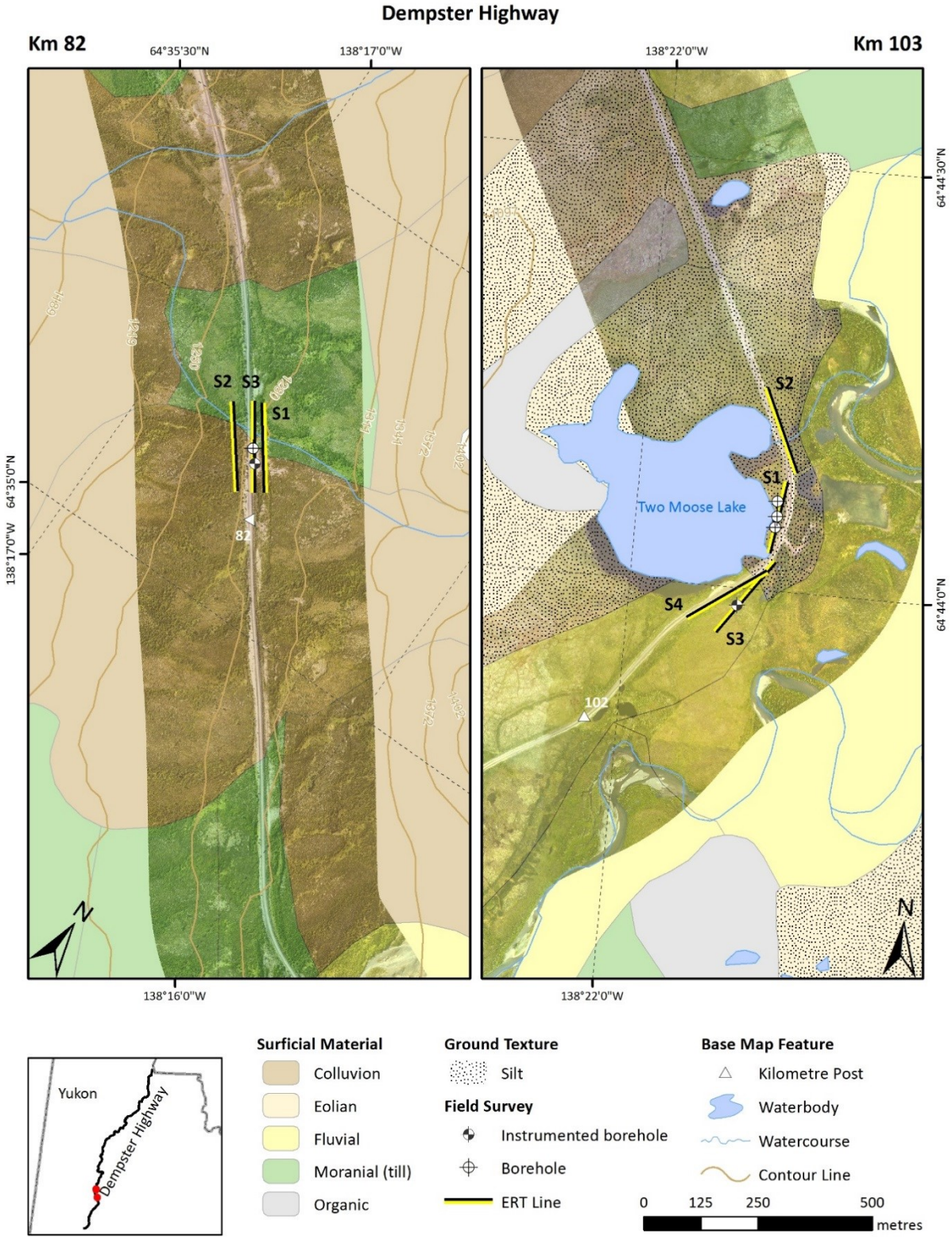

Figure 2.2. Figure 2: Surficial geology at km 82 and 102.

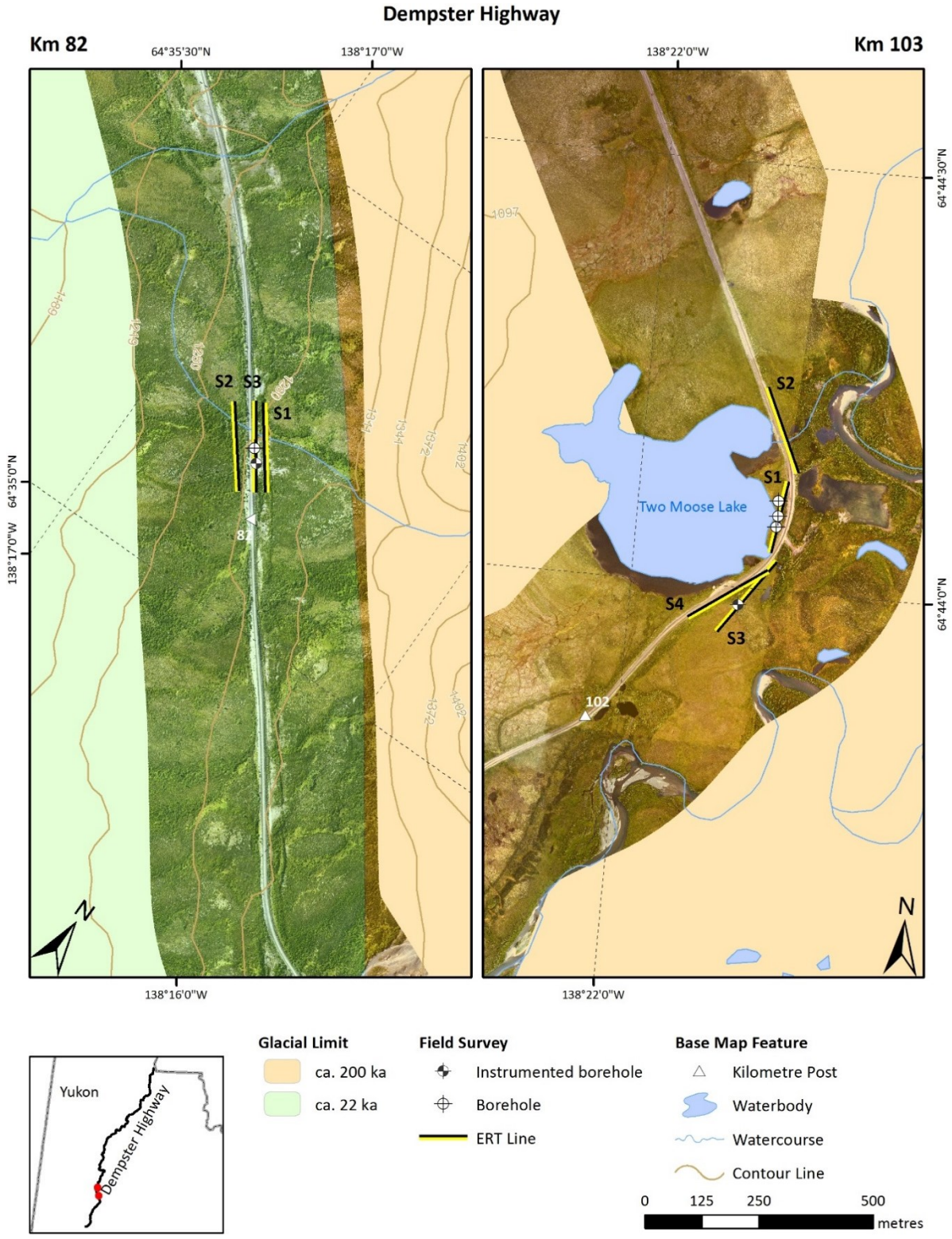

Figure 2.3 Glacial limits at km 82 and km 102.

3. METHODOLOGY

The objective of this project was to understand the issues contributing to the formation of sinkholes at km 82 and 103 of the Dempster Highway. To achieve this objective, a combination of desktop study and field investigation were used.

3.1 Assessment of existing data

Surficial geology maps prepared by the Yukon Geological Survey, as well as aerial and satellite images were interpreted as part of this project. These data were supplemented with geotechnical reports from consultants and discussion with civil engineers and maintenance crew from HPW. Data and personal communications were combined, analyzed and interpreted to complement previous efforts.

3.1.1 Field Surveys

Field investigation was focused largely on the acquisition of new geophysical information using electrical resistivity tomography (ERT) surveys. In addition, shallow drilling was used to verify interpretations of geophysical information and to develop cryostratigraphic logs. Importantly, the work focuses on areas proximal to the highway embankment either in the field parallel to the highway, or at the toe and on the shoulder of the embankment, where minimal information is currently available. This information is key because it will allow project researchers to infer the probability of permafrost presence under the highway embankment.

3.1.2 Electrical Resistivity Tomography

Electrical resistivity tomography (ERT) is a geophysical method that passes electrical current through stainless steel electrodes that are driven into the ground surface. A central “station” measures the resistivity distribution of the subsurface between electrode pairs. Resistivity is the mathematical inverse of conductivity and indicates the ability of an electrical current to pass through a material. Mineral materials (with the exception of specific substances such as metallic ores) are mostly non-conductive. Therefore, variation in the resistivity of a soil or rock profile is governed primarily by the amount and resistivity of pore water present in the profile, and the arrangement of the pores. This makes ERT very well suited to permafrost and hydrology applications. Because most water content in frozen ground is in the solid phase and typically has a higher resistivity than unfrozen water content, permafrost distribution can be inferred based on changes in resistivity between frozen and unfrozen ground.

An ERT system consists of an automated imaging unit and a set of wires connected to an electrode array. The system used for the surveys presented in this report is an ABEM Terrameter LS electrical resistivity and tomography system, consisting of a four-channel imaging unit and four electrode cables, each with 21 take-outs at five-metre intervals. To conduct a survey, 81 electrodes are driven into the ground along a survey line and connected to the electrode cables (Figure 3.1).

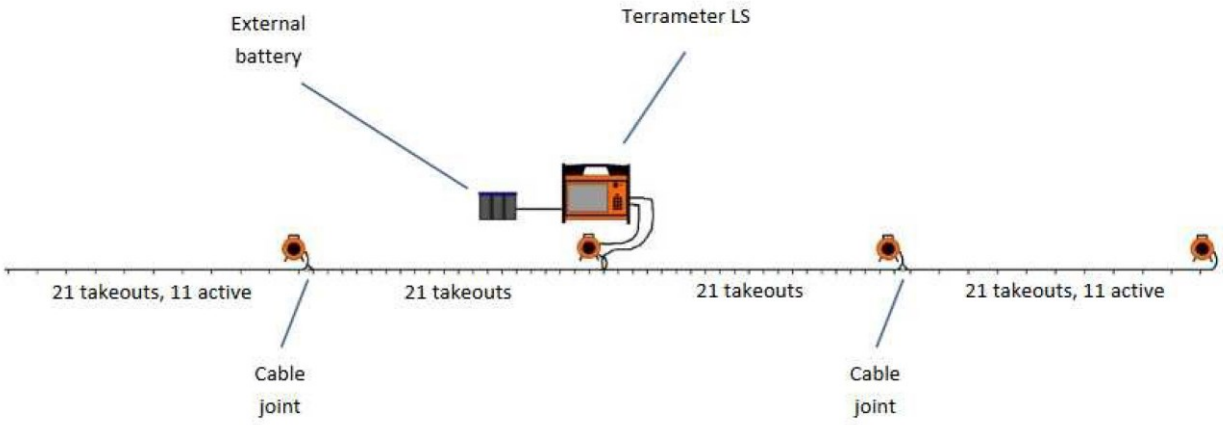

Figure 3.1. Instrument set-up for ERT surveying.

Three different types of electrode configurations or arrays were used during the surveys: the "Wenner", "Dipole-dipole", and "gradient" arrays. These arrays differ in how they pair current and potential electrodes (Figure 3.2). A direct current electrical pulse is sent from the resistivity meter along the survey line in two current electrodes (C1 and C2), and the measurement is performed by two potential electrodes (P1 and P2). The resulting data consists of a cross-sectional (2D) plot of the ground's resistivity (ohm.m) versus depth (m) for the length of the survey.

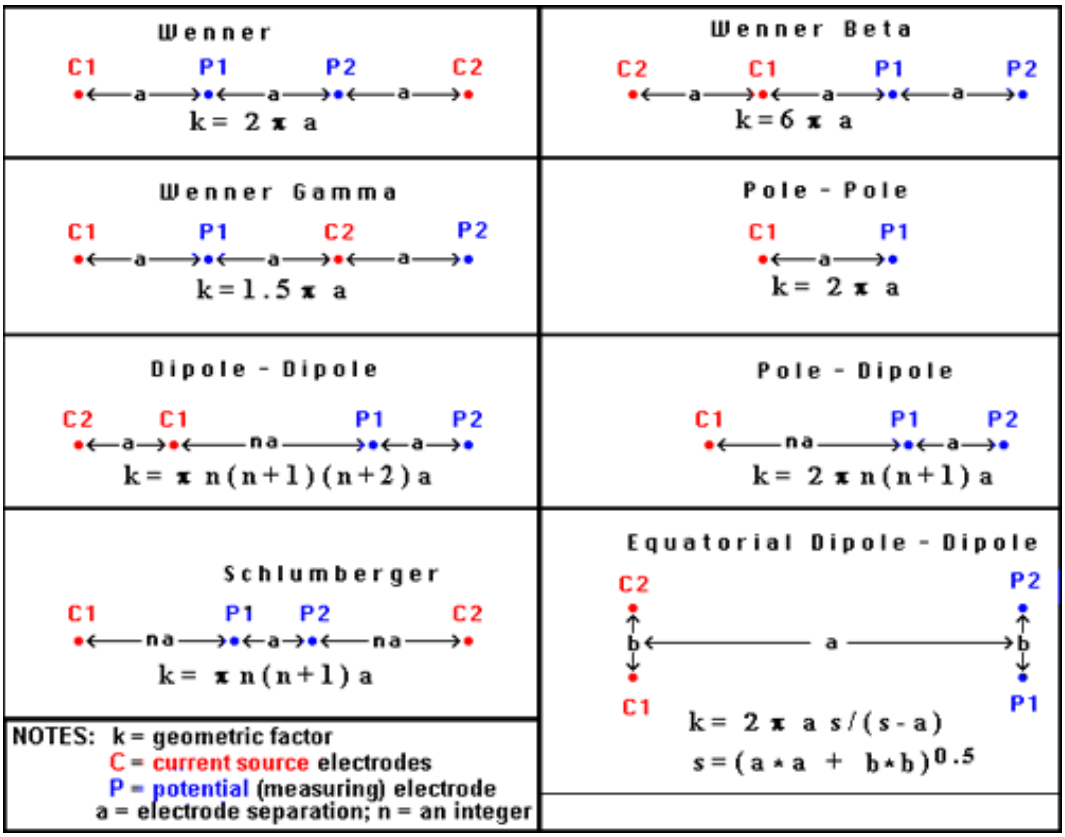

Figure 3.2. Survey configurations or "arrays" for ERT surveying.

In general, the Wenner array is good in resolving vertical changes (i.e. horizontal structures), but relatively poor in detecting horizontal changes (i.e. narrow vertical structures). Compared to other arrays, the Wenner array has a moderate depth of investigation. Among the common arrays, the Wenner array has the strongest signal strength. This can be an important factor if the survey is carried in areas with high background noise. Relatively small current magnitudes are needed to produce measurable potential differences. The disadvantages are that in order to image deep into the earth, it is necessary to use longer current cables. The Wenner array is also very sensitive to near surface inhomogeneities which may skew deeper electrical responses. One disadvantage of this array for 2-D surveys is the relatively poor horizontal coverage as the electrode spacing is increased, which can be a problem when using a system with a relatively small number of electrodes.

The dipole-dipole array is very sensitive to horizontal changes in resistivity, but relatively insensitive to vertical changes in the resistivity. That means that it is good for mapping vertical structures, such as dykes and cavities, but relatively poor in mapping horizontal structures such as sills or sedimentary layers. This array can have a shallower depth of investigation compared

to the Wenner array, but it has better horizontal data coverage than the Wenner, which can be an advantage when the number of nodes available with the multi-electrode system is small. One possible disadvantage can be a very small signal strength. With the proper field equipment and survey techniques, this array has been successfully used in many areas to detect structures such as cavities where the good horizontal resolution of this array is a major advantage.

The “gradient” array is similar to the Wenner array, but with asymmetrical electrode pairs. The “Gradient” array is less conventional, but was tested due to its efficiency and fast data acquisition time. Compared together, the data obtained by the three types of surveys allow a more comprehensive interpretation of each study sites.

Results of the surveys are post-treated and analyzed at the NCE using inversion software (Res2DInv 64 and Res3DInv 32).

3.1.3 Permafrost drilling and sample collection

A light and portable GÖLZ Earth-drill system was used to drill shallow boreholes. The borehole was initiated by shoveling a fore hole down to the thaw front. At the thaw front, the Earth-drill system was used. The drill uses a small Stihl engine with a high-speed transmission (600 rpm). The drill is coupled to stainless steel rods (1 metre in length and 4.5 cm in diameter) and a core barrel (40 cm long and 10 cm in diameter) with diamonds set in carbide alloy teeth. The drill is used in unconsolidated, fine to medium-grain material (sand to clay). A core catcher tool was used to extract frozen core from the borehole, allowing for the collection of continuous, undisturbed permafrost samples. This type of drilling is limited to a maximum drilling depth of approximately 5 to 6 m under optimal conditions. To drill boreholes at deeper depths, a conventional water-jet diamond drill was used. Details regarding these tools and the drilling methodology are provided in Calmels, Gagnon and Allard (2005).

The same sampling and drilling protocols were followed for each borehole. The site was first described (e.g., hydrology, vegetation type and density, topography), photos were taken, and locations were recorded using a hand-held GPS. Each core sample was photographed and described in situ (e.g., soil type, soil moisture, presence or absence of organic matter, any notable features). Each sample extracted from a borehole was identified by borehole name and depth. Samples were put in polybags and sealed immediately after being extracted. Samples were kept frozen and stored in a freezer that was taken back to the laboratory for further analyses. In the laboratory, each core was cleaned with cold water to remove drilling mud and then photographed.
In addition, HPW had two additional boreholes drilled by a contractor in September 2014 (#841-4949) and September 2015 (#876-5321). The boreholes were drilled and sampled to the depth

of 7.3 m and 13.7 m respectively. The samples were photographed and described on site and then were brought back to HPW laboratory facilities for grain-size and water content analyses using their own methodology (not detailed in this report).

3.1.4 Permafrost sample analysis

Laboratory analyses were carried out to measure the properties of the permafrost samples. Both soil grain characteristics and ice characteristics were evaluated. To evaluate soil grain characteristics, a grain-size analysis was performed on selected samples. To evaluate ice characteristics in permafrost samples, the cryostructure, volumetric ice content and gravimetric ice content were quantified. These methods are described below. For more information, please refer to Andersland and Ladanyi (2004).

Grain-size analysis

Sieve and hydrometer analyses of grain size were performed following a specifically modified American Standard and Testing Method protocol (ASTM D422-63, 2000). The sieves used were 4, 2, 1, 0.5, 0.25, 0.125 and 0.063 mm.

Cryostructure

Permafrost cryostructure (the geometry of the ice in the permafrost) depends on water availability, the soil's ice-segregation potential, and the time of freezing, all of which affect the development of ice structures in the soil matrix. Information such as soil genesis, climate conditions at the time of freezing, permafrost development history, and ground vulnerability when permafrost degrades can be interpreted from cryostructure (the shape of the ground ice), cryofacies (groups of cryostructures) analysis, and general cryostratigraphy (assemblages of cryofacies).

Because field descriptions are based only on a visual interpretation of the core, the samples were described a second time more thoroughly in the laboratory using standard terminology (Murton and French 1994). Frozen core samples were warmed to near 0°C and any refrozen mud was scraped off before the sample was described.

Gravimetric ice content

Ice content was calculated using:

$$u1 = \frac{(M_i)}{(M_s)}$$

where M_i is the ice weight, measured as weight loss after drying (g), and M_s is dry soil weight in grams. Results are expressed as percentages (dimensionless).

Volumetric ice content

The volumetric ice content was calculated by immersing the frozen sample, bagged in vacuum-sealed polybags, in a recipient to measure its volume (Vtot). The sample was then thawed and put in the oven to dry. The remaining dry material was immersed again to determinate its volume (Vsed). The volume of excess content was calculated using:

$$V_{tot} - V_{sed} = V_{ice}$$

The volumetric ice content is expressed as percentages (fundamentally meaning cm^3/cm^3).

3.1.5 Borehole logs

A log for each permafrost borehole was created by assembling laboratory photos of the cores. Borehole logs include maximal depths, grain size ratio and volumetric ice content. These logs were used as supporting data for mapping.

3.1.6 Ground temperature and climate monitoring

The newly-drilled borehole at km 102-103 was instrumented to monitor ground temperature at the end of July 2016. To do so, a HOBO (U12-008) four-channel external data logger was used. This stand-alone weatherproof logger can record data at various intervals and uses a direct USB interface for fast data offload. The logger requires one three-volt CR-2032 lithium battery. Each battery will typically last one year when logging intervals are greater than one minute. To ensure uninterrupted operation, the data loggers were placed in a sealed 15-cm x 15-cm junction box that was connected to the borehole casing. All borehole casings were made of electrical-grade PVC filled with silicone oil. The temperature sensors (TMC6-HD to TMC50-HD) can accurately record temperatures ranging from –20°C to +70°C, with interchangeability to a tolerance of +/–0.25°C from 0°C to 50°C. They have a resolution of 0.03°C at 20°C.

The ground surface temperature was monitored using the HOBO Pendant data logger (UA-002-08). This miniature waterproof two-channel data logger can accurately record temperatures ranging from –20°C to +70°C with interchangeability to a tolerance of +/– 0.53°C from 0°C to 50°C. The UA-002-08 loggers have a resolution of 0.14°C at 25°C.

The second borehole (#876-5321) drilled at km 82 was instrumented by HPW in late November 2015. During our analysis of the data, it appeared that one of the thermistor had been impaired and was not logging temperature properly. The damaged cable was repaired and the site appears to be fully operational as of July 24th 2016.

4. PREVIOUS SURVEYS

In October 2014, GroundTruth Exploration was contracted to investigate km 82 of the Dempster Highway, because extensive cracks and sinkholes had been forming. A high resolution electrical resistivity survey was used in conjunction with high resolution aerial imagery collected using an unmanned aerial vehicle (UAV) to attempt to understand the reason for the subsidence at this location, and use this knowledge to predict zones susceptible to future subsidence.

The resistivity profile in Figure 4.1 shows the known sinkholes and surrounding areas of subsidence at and around electrode 84, and above the culvert at electrode 116. Both locations showed a similar pattern with a vertical band of low resistivity extending to depth cutting through higher resistivity ground.

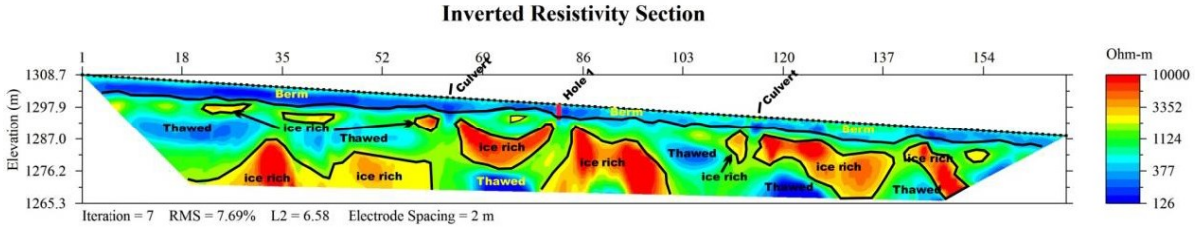

Figure 4.1. DC resistivity profile at KM82 (from GroundTruth Exploration, 2015)

The causes of these sinkholes were not identified in this report, mainly due to the lack of ground truthing data which is usually used to link the soil stratigraphy with resistivity values. However, there was evidence that the high resistivity pockets may be concurrent with drainage features on the hillside, thus leading to the conclusion there may be ice-rich permafrost under them.

Later, DMT Geosciences was contracted by the Government of Yukon Transportation and Engineering Branch (TEB) to conduct geophysical surveys along the Dempster Highway to assess the condition of the permafrost beneath the highway from km35 to 36.5 and km71.5 to 130). Ground Penetrating Radar (GPR) and OhmMapper data were collected in one pass in both the north and southbound lanes of the areas of interest. From this data, an additional seven targets were chosen for investigation using Multichannel Analysis of Surface Waves (MASW), a seismic survey technique. This survey was carried out from June 14th to July 7th, 2015. No drilling or ground temperature monitoring was completed as part of either the DMT Geosciences or the GroundTruth Exploration analyses.

Figures showing the processed and inverted data for each kilometer of highway surveyed were provided. Km 82 was interpreted as an area with pockets of possible high ice content 10-30m wide and occasional areas of possible high ice 100-300m wide (Figure 4.2). It needs to be acknowledged that using OhmMapper data, there are limits to the resolution of the geophysical methods employed. The resolution that can be achieved depends on thickness, depth of burial and contrast of the various layers and bodies relative to the parameters such as spread length and receiver spacing used in the geophysical surveys.

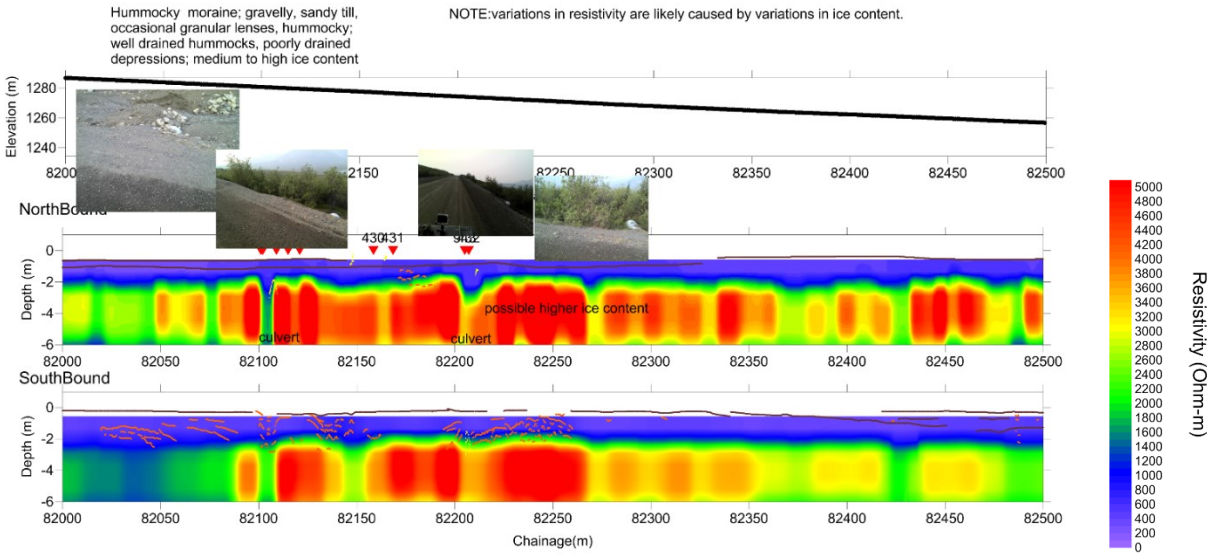

Figure 4.2. DC resistivity and GPR profiles at KM82 (from DTM Geosciences Ltd., 2015)

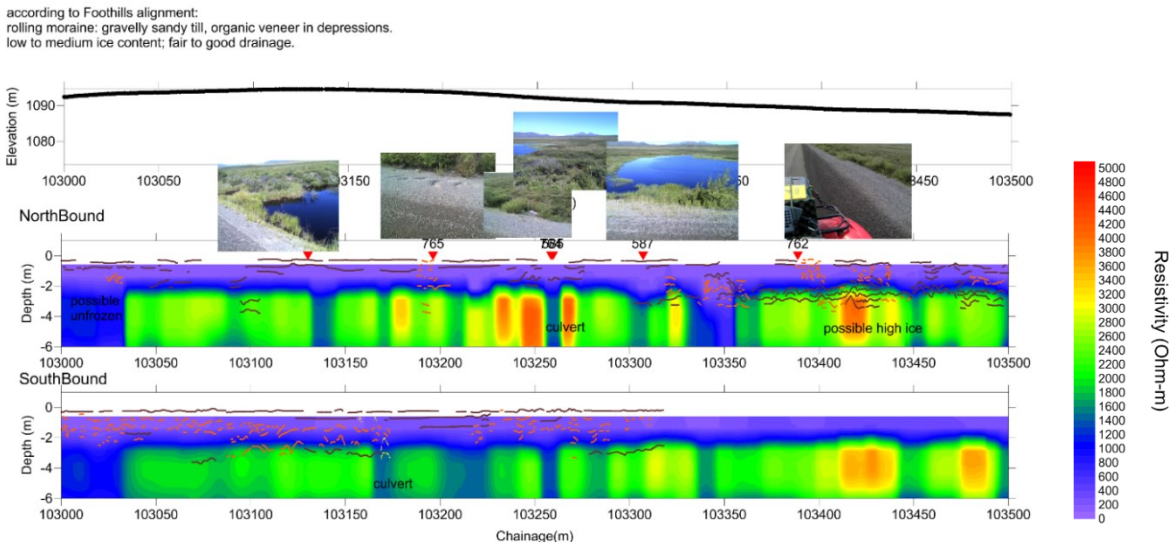

Figure 4.3. DC resistivity and GPR profiles at KM103 (from DTM Geosciences Ltd., 2015)

Km 102-103 was interpreted as an area with lower resistivity with a few small possible high ice areas and several possible unfrozen areas (Figure 4.3). It was noted that due to the lack of borehole data, it might be necessary to revisit the interpretation once more drill control is obtained and calibrate the assumptions better to local conditions. The MASW interpretation would benefit from the input of geotechnical information.

5. RESULTS

5.1 Km 82

5.1.1 Summary of data collection

Potential causes for the sinkholes at km 82 were investigated using 3 ERT survey lines (Figure 5.1). Survey 1 (S1) was located in the field, parallel to the road on the right-hand side (RHS), 34 m from the centerline. It was used to assess permafrost upslope from the road and out of the influence of the embankment. Survey 2 (S2) was also located in the field, parallel to the road and 34 m from the centerline, but at the left-hand side (LHS) of the road. It was used to assess permafrost downslope of the road and out of the direct influence of the embankment. This survey crossed a depression that may have resulted from permafrost thaw (figure 5.2). Finally, survey 3 (S3) was located on the RHS, 9 m from the centerline. This survey crosses directly over the area that has been affected by the sinkhole processes. S3 was parallel to the road, and passed above the boreholes 841-4949 and 876-5321 which were drilled in 2014 and 2015, respectively. It was used to assess permafrost in the most disturbed area and to compare ERT data with borehole logs and the ground temperature recorded in borehole 876-5321. The logs and geotechnical analyses of each borehole were available and are presented and discussed further below. Borehole 876-5321 included temperature sensors at 8 depths. One of the temperature sensor cables was cut by wildlife during the winter, and repaired on site by the research team during the field investigations. At the time of the survey, no damage was observed on the road, on its shoulders, or at the toe of the embankment.

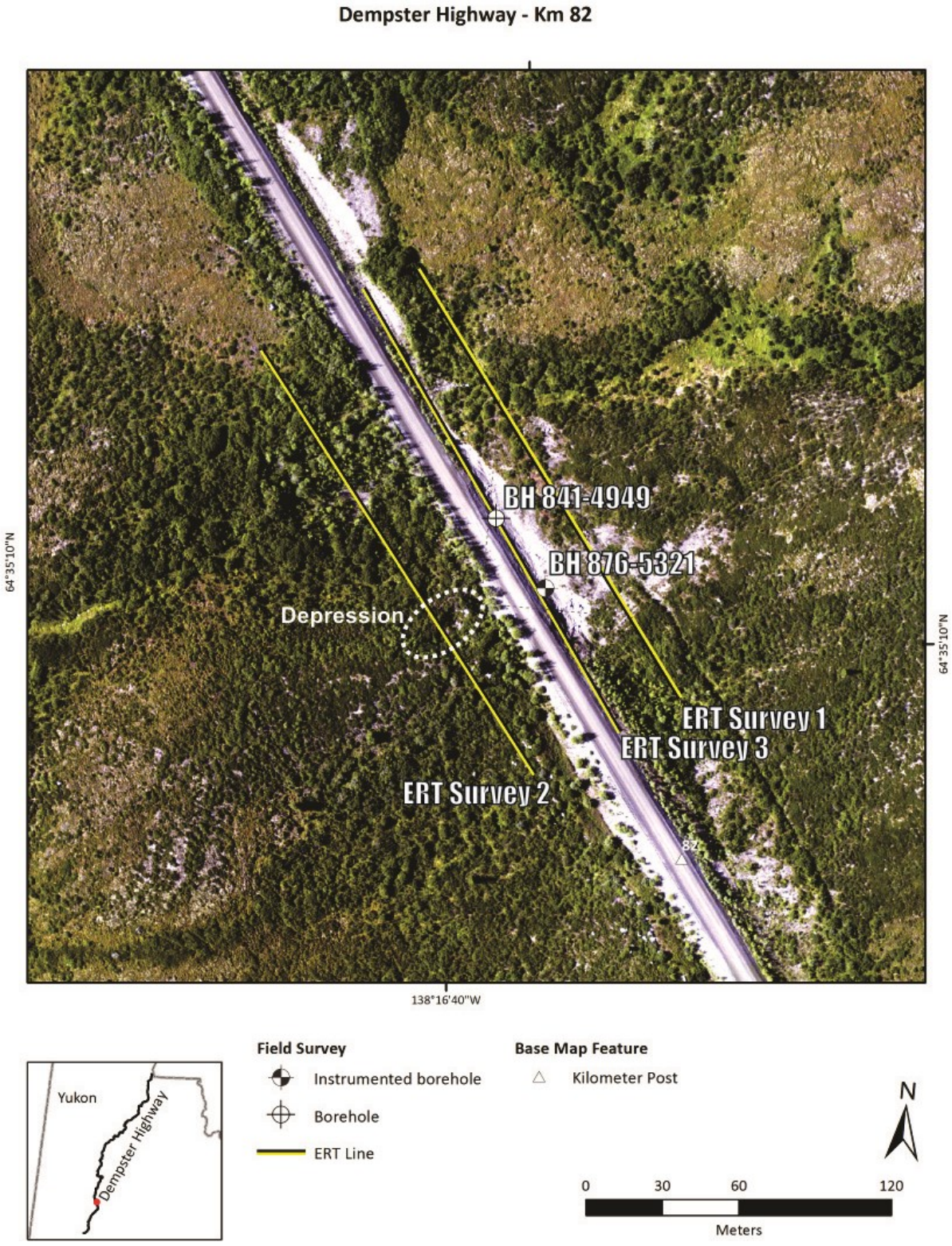

Figure 5.1. Air photo showing km 82 study site with location of the ERT surveys, boreholes, and noticeable features.

Figure 5.2. Depressed area with collapsing at the LHS.

5.1.2 Borehole data

Logs

Prior to this project, two boreholes were drilled by contractors for HPW. Borehole 841-4949 was drilled September 30th 2014, and reached the depth of 7.3 m. Borehole 876-5321 was drilled one year later September 27th 2015, and reached 13.7 m depth (Figure 5.3). While the climate conditions each year may have differed, both were drilled at the same time of the year, and it can be assumed that the thaw front was close to its maximum depth when both holes were drilled. Permafrost was reported at 6 m depth in 841-4949, while no frozen ground was reported down to the maximal depth of 13.2 m in 876-5321. Yet, the ground temperature records (presented in the next section) show that the ground is frozen at 13.2 m, and it may be frozen above, at about 10 m. The potential that the drilling process thawed the cores and significantly disturbed the ground thermal regime cannot be excluded, especially if the ground temperature was close to 0°C, and the soil was coarse and ice poor. The grain size distribution

of the soil in 841-4949 consisted of silty sand with gravel, the grain size distribution being constant along the profile. In 876-5321 the soil was also silty sand with gravel near the surface but evolved into a gravel with silt and sand with depth, with a maximal gravel content of 65.3% at about 7 m, and then progressively revert to silty gravel with sand at about 9 m and a silty sand with gravel at about 10.5 m (Figure 5.3).

The two boreholes are about 35 m apart – close enough that similar stratigraphy would be expected for the two. However, borehole 876-5321 shows an impoverishment in fine sediment from about 3 to 10 m, while the ratio remains constant in 841-4949 all along the profile. In the absence of other obvious causes, this suggests that fine sediment have been leached out at 876-5321, the location where sinkholes have occurred, but not in 841-4949. Another interesting fact is that no ground ice was sampled in either borehole, even in still frozen material.

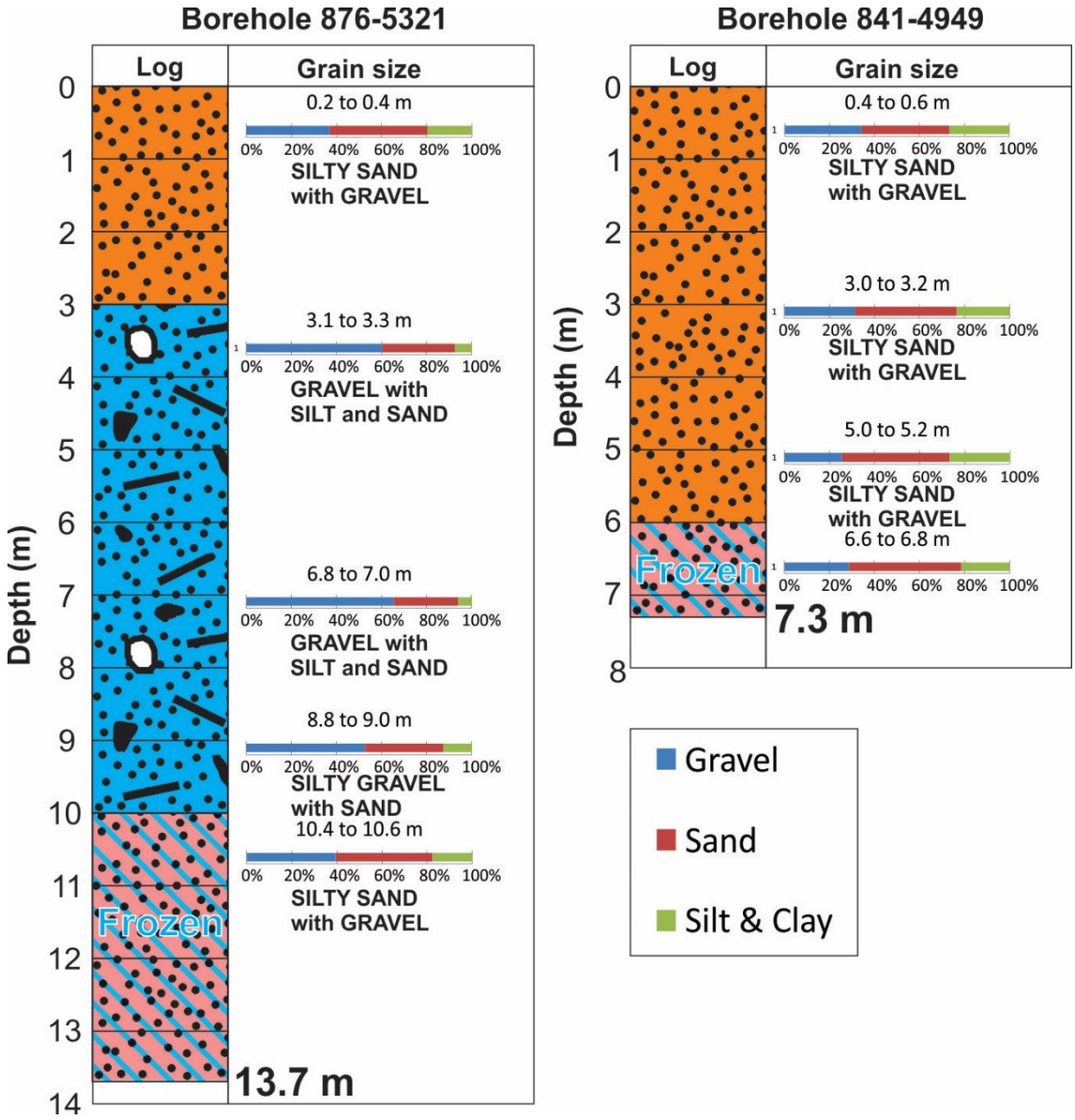

Figure 5.3. Logs for boreholes 841-4949 and 876-5321 with grain size distribution

Ground temperature

Ground temperature records were recorded from December 2015 to August 2016 in borehole 876-5321 (Figure 5.4). Monthly mean ground temperature profiles show that the base of the borehole is frozen, at or slightly below 0°C (Figure 5.4A). Temperature at 10 m remains close to 0°C with moderate oscillation – within the range of the sensor accuracy (±0.25°C). Nevertheless, temperature curves for each depth show a clear increase above 0°C late in May 2016 at 8 and 10 m depths (Figure 5.4C). While the temperature at 10 m decreases after May and remains stable, the temperature at 8 m decreases and then rises again at the end of August 2016. The borehole may still be recovering from the drilling disturbance so interpretations are tentative, but we infer that the permafrost top would be located at about 10 m depth in the absence of drilling disturbance. It will be possible to verify this interpretation using additional yearly records. Above the permafrost top, the initial general increase of ground temperature is observed in May at the time of the freshet propagating from the surface to the lower depths.

Higher frequency variation of temperature observed in the curves for shallower depths (Figure 5.4C) can be attributed to air temperature variations and the infiltration of ground water originating from freshet and precipitation. Unfortunately, there are not sufficient climate data available to allow comparison between ground temperature and precipitation records. Figure 5.5 presents ground temperature recorded at km 82 at 0 and 0.5 m with precipitation in Dawson City for June, July, and August 2016. A relationship appears to exist between temperature and precipitation peaks, with a delay of the precipitation of one to three days. This apparent relationship implies that: 1- precipitation has a major warming effect on the temperature profile at the site; and 2- the high reactivity of the temperature profile suggests high permeability as underground water seems to flow relatively quickly.

In summary, the investigation of borehole logs, ground temperature and climate records indicate that ground water movement in the active layer is warming ground temperature and may be inducing permafrost thaw. It may also be responsible for leaching of fine sediment.

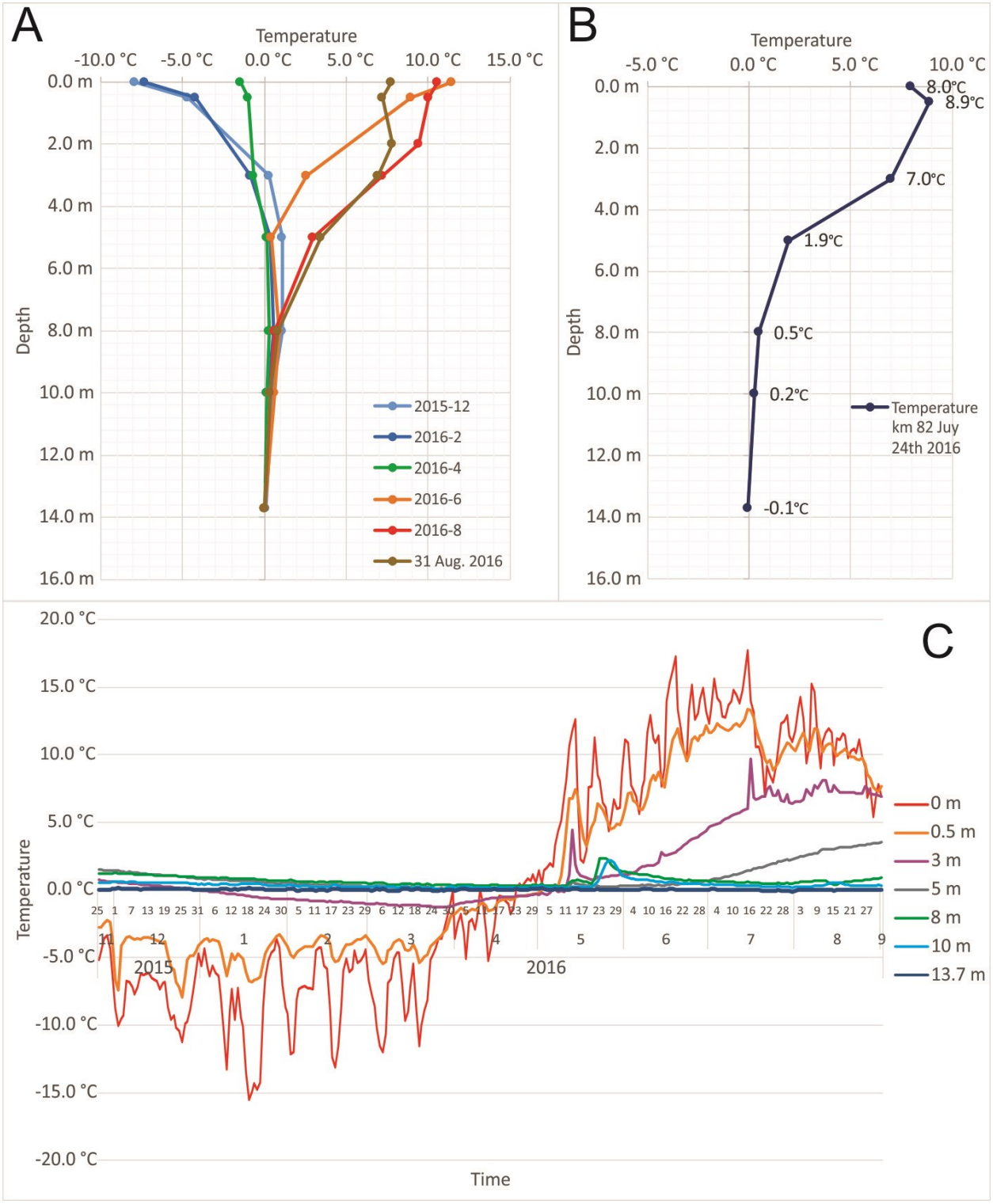

Figure 5.4. Ground temperature at km 82. A- Monthly mean temperature profiles; B- temperature profile at time of ERT survey 3; C- ground temperature curves at 0, 0.5, 3, 5, 8, 10, and 13.7 m.

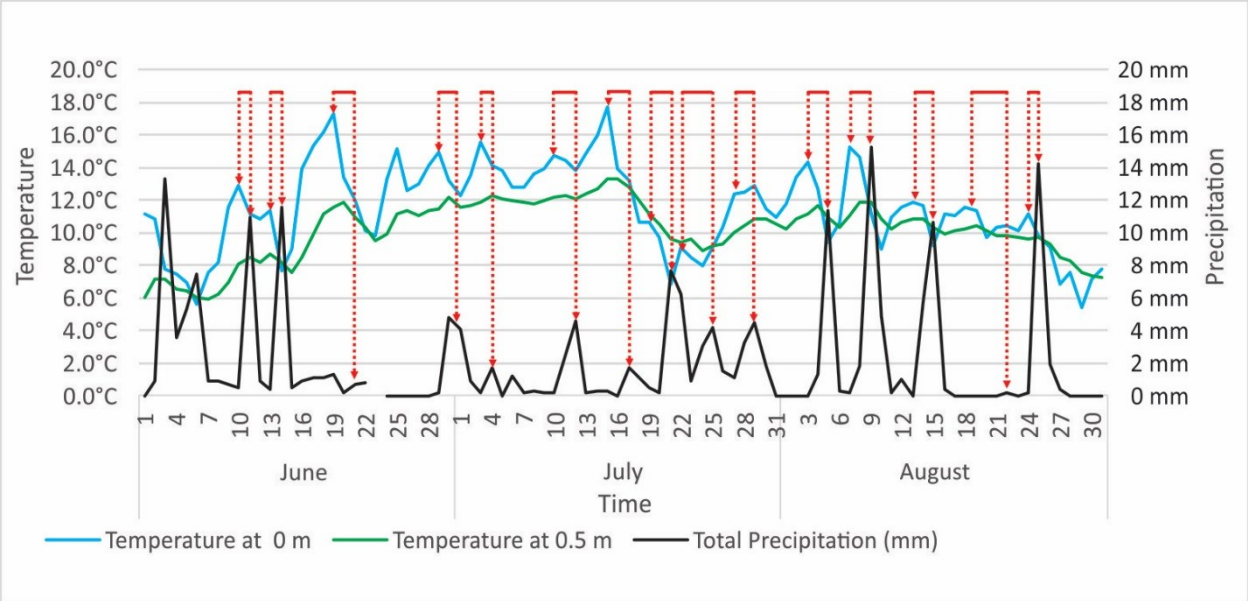

Figure 5.5. Ground temperature recorded at km 82 at 0 and 0.5 m and precipitation in Dawson City for June, July, and August 2016.

5.1.3 ERT surveys

The results of the ERT surveys are presented in Figures 5.6, 5.7, and 5.8. They are presented from the LHS on the top to the RHS to the bottom, the profile being oriented South to North. This makes a visual, spatial comparison possible, yet the profiles are discussed in a different order, starting upslope, from the least disturbed site, and moving downslope.

Survey 1 – RHS – field - 34 m from the centerline

Wenner array - Survey 1 (Figure 5.6): The survey is located upslope of the road to be as far away from the impacts of the embankment and its modification of hydrology and snow accumulation. This survey is the most likely capture the characteristics of an undisturbed permafrost environment. The ERT profile shows two high resistivity values areas, one between chaining 70 and 140 m, in the upper part of the profile between 0 and 4 m depth, and the second at the North end of the profile between 10 and 20 m depth. For the rest of the profile, resistivity values range from 600 to 1100 ohm.m. Between chaining 12 and 76 m resistivity is between 1000 and 1100 ohm.m from 6 to 20 m depth. This could be due to coarser sediments, colder ground temperatures, or higher ice-content. However, these values are too low to be an indicator of a massive ice body.

Dipole-dipole array - Survey 1 (Figure 5.7): This dipole-dipole survey shows three areas of high resistivity. Starting from the south high resistivity was between one between chaining 15 and 45 m (surface to 15 m depth); from chaining 75 to 95 m (7 to 15 m depths; 2000+ ohm.m resistivity core), and at the northern end of the profile. The second and third areas are consistent with higher resistivity areas observed in survey 3, but the resistivity value are lower.

Gradient array - Survey 1 (Figure 5.8): The ERT profile shows many similarities with the dipole-dipole profile. There are also three high resistivity values areas located in the same locations., however, resistivity values are slightly lower.

Survey 3 – RHS – foot of the embankment – 9 m from the centerline

Wenner array - Survey 3 (Figure 5.6): This survey passes above the location of both boreholes, at chaining 58 and 98 m along the survey line (from the south) making it the only one that allows comparison between the geophysical and borehole data. The temperature profile recorded at borehole 876-5321 presented in Figure 5.4B indicates that the permafrost table was located between 10 and 13.7 m depth. The resistivity values between these two depths at the borehole locations range from about 800 to 1000 ohm.m. Deeper in the profile, resistivity values remain below 1300 ohm.m. Overall the resistivity values are relatively low for a frozen coarse sediment. This may imply that if permafrost still is present at these locations, it is quite warm, close to 0°C, with relatively high liquid water content. The profile does not suggest the presence of massive ground ice, as the resistivity values are relatively low.

Dipole-dipole array - Survey 3 (Figure 5.7): If we consider that the temperature profile recorded at borehole 876-5321 indicates that the permafrost table was located between 10 and 13.7 m depths at the time of the survey, the resistivity value between these two depths at borehole location range from about 600 to 1000 ohm.m. This is slightly less resistive than what was measured using the Wenner survey. The dipole-dipole survey shows a higher resistivity area located between chaining 70 and 110 m, with resistivity higher than 3000 ohm.m at chaining 90 m, at 16 m depth. Below this depth, resistivity progressively decreases. Anywhere else, resistivity remains relatively low, except in the North end of the profile. The high resistivity area can be an indicator of ice richer ground or the presence of a bedrock spur or possibly the presence of coarser or colder material.

Gradient array - Survey 3 (Figure 5.8): Again, considering that the temperature profile recorded at borehole 876-5321 indicates that the permafrost table was located between 10 and 13.7 m depths at the time of the survey; the resistivity value between these two depths at borehole location range from about 700 to 900 Ohm.m. This is similar in magnitude to the two previous surveys. The gradient survey also shows a higher resistivity area located between chaining 70

and 110 m, but the resistivity value reached a maximum of 2000 ohm.m. This was lower than what was measured using the dipole-dipole survey. Higher values are observed at chaining 86 m, at about 20 m depth. Below this depth, resistivity decrease progressively. Anywhere else, resistivity remains relatively low, except at the North end of the profile, as observed in the dipole-dipole survey.

Survey 2 – LHS – field - 34 m from the center line

Wenner array - Survey 2 (Figure 5.6): The survey is located downhill. Though the survey is in the field, the embankment may have had an impact because it intercepts runoff, channelizes water through a culvert, and the thaw of permafrost below the embankment may have opened new pathways for underground water flow. These factors may have an effect on terrain located at lower elevations.

The ERT profile shows three high resistivity areas, starting from the south:

1. Between chaining 10 and 35 m from the surface to about 10 m depth;
2. Between chaining 65 and 95 m with a 1800+ ohm.m resistivity core between about 7 and 15 m depths;
3. At the northern end of the profile with resistivity values reaching 2000+ ohm.m at depth that exceed the boundary of the profile.

An area of near-surface low resistivity mainly matches the zone where depressions were observed.

There are two possible explanations for these observations. Either the high resistivity values are attributable to the presence of ground ice and its melt resulted in the depression and collapse observed in the field, or the high resistivity values are attributable to a gravelly sediment that have had fine material leached out, resulting in surface collapse. In both cases, this problematic area does not seem to extend deeper than 20 m.

The bulbs with the highest resistivity values are located close to the surface; the values progressively decrease with depth. This can be an artefact attributable to the ERT survey itself. Alternatively, it could be consistent with either high concentration of ground ice close to the surface, or more fine-impoverished gravel close to the surface because of leaching/water seeping processes.

Dipole-dipole array - Survey 2 (Figure 5.7): As noted in the analysis of the Wenner survey, the ERT profile shows three high resistivity values areas at the same locations. The first, located at the southern end of the profile appears to be less resistive than what was measured with the Wenner array, but is spread over a greater area; it remains relatively shallow. The second high resistivity bulb, between chaining 70-80 m, shows higher resistivity values, around 6000 ohm.m

than what was measured with the Wenner array. A core of 2000-6000+ ohm.m is present between 3 to 15 m depths. The third resistive area is located at the north end of the survey. It has resistivity values of ≈4000 ohm.m. This survey discriminated 2 resistive areas between chaining 170 and 180 m; one located between 2 and 8 m depths, and a second starting at about 15 m depth. The three high resistivity areas are consistent with those observed in the other dipole- dipole surveys (S1 and S3). The high resistivity bulb in the chaining 70-80 m area shows the same pattern as the Wenner survey, with higher values close to the surface then decreasing values with depth. Resistivity values are higher than the corresponding parts of dipole-dipole surveys 1 and 3.

Gradient array - Survey 2 (Figure 5.8): The gradient survey is very similar to the dipole-dipole; it shows three areas with high resistivity values. The location and observations for this survey are the same as those for the corresponding dipole-dipole survey. The biggest difference between the two surveys is that the resistivity values shown by the gradient survey are generally lower than those of the dipole-dipole. For example, 6000 ohm.m resistivity in the dipole-profile corresponds with resistivity of 4000 ohm.m in the gradient profile. The Wenner profile resistivity values are even lower, with maximum resistivity values of about 2000 ohm.m.

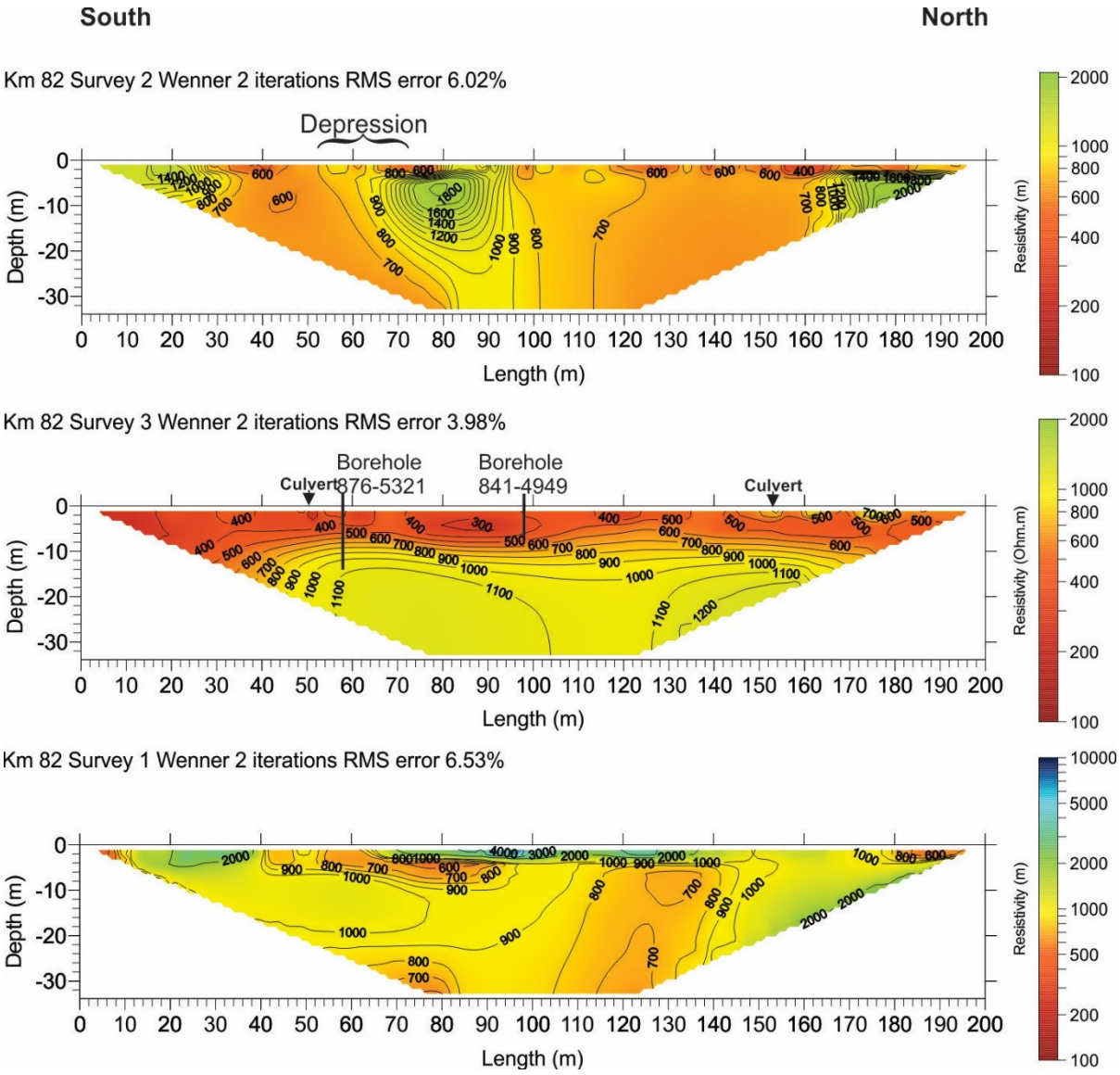

Figure 5.6. Wenner ERT surveys at km 82.

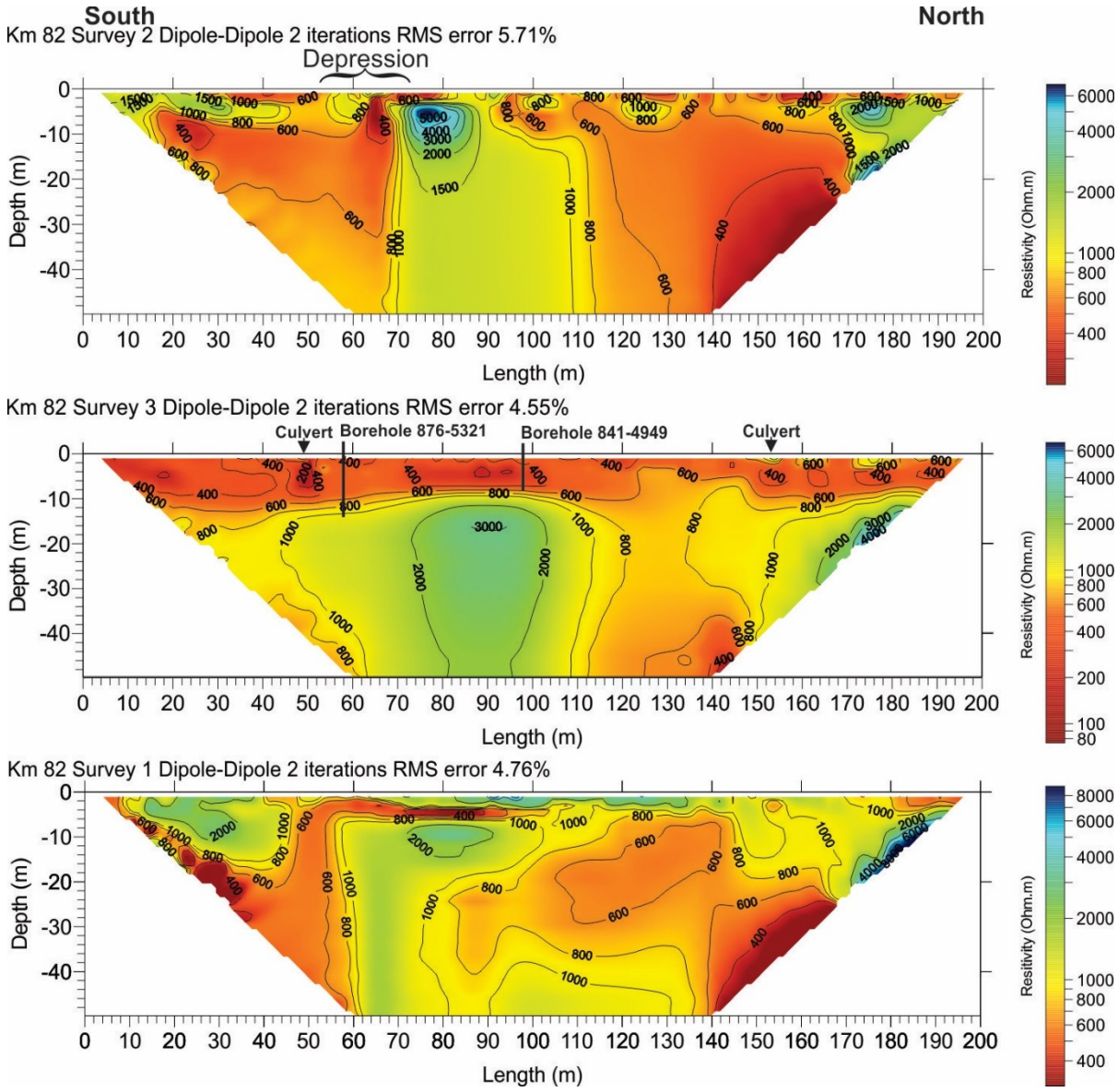

Figure 5.7. Dipole-dipole ERT surveys at km 82

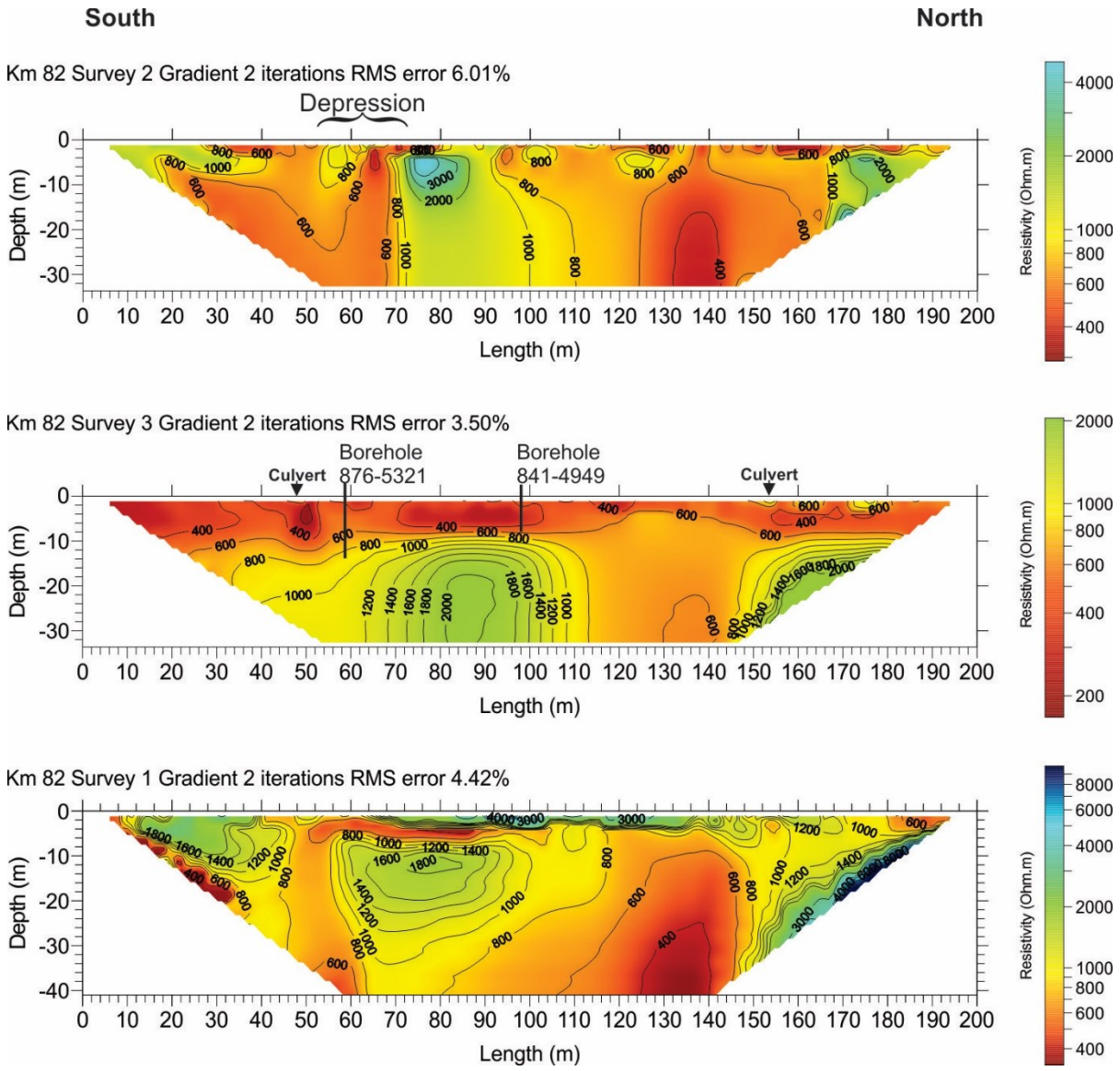

Figure 5.8. Gradient ERT surveys at km 82

5.2.3 Interpretation

The localized decrease of fine material content observed in the borehole log 876-5321 versus stable fine content in borehole log 841-4949 suggest leaching of sediments by ground water.

No ground ice was sampled or reported in either borehole; this suggests that ground ice melt is not the cause of the observed subsidence and subsequent sinkhole formation.

Ground temperature profiles suggest a thermal effect of subsurface water movement on ground temperature. Comparison with precipitation records from Dawson City Airport, 80 km away, suggests that the infiltration can be fast and that there might be a flow sufficient to either thermally erode permafrost and/or leach out fine sediment particles.

ERT resistivity values are generally relatively low, consistent with an ice-poor permafrost. Tge low resistivity does not support the hypothesis of a thawing massive ice body as the cause of subsidence. However, some highly resistive areas may indicate either a more ice-rich permafrost or a coarser sediment, at locations.

ERT surveys carried in the field generally show lower resistivity values deeper in the profile. At the survey done along the road (S3), low resistivity values are concentrated in the upper parts of the profile and the higher in the lower parts. These observations may indicate that the upper ground is likely permafrost free at the toe of the road due to the impact of the embankment. By comparing ground temperature records from the borehole and resistivity values measured at the same depth, it is likely that areas with resistivity values below 600 to 800 ohm.m (depending on the type of survey array) are not frozen.

The fact that sediment is generally gravely, with ground temperature very close to 0°C suggests that, where present, permafrost is highly vulnerable to thawing.

Results from the ERT surveys could support either of the two hypotheses for causes of sinkhole formation (i.e., either fine material being leached away, or ground ice being melted). However, the borehole data favor the leaching hypothesis. In both cases permafrost degradation is the contributing to the issue. The presence of snow accumulating on the shoulder of the embankment may have promoted a thickening of the active layer. The retreat of the permafrost table may have open new pathways for the ground water originating from precipitation to flow through sediment and leach sediments. Similarly, an increase of the precipitation in the area over decades may have led to the situation. Ground temperature records have proven that infiltrated water are significantly impacting permafrost on this site.

5.2 Km 102-103

5.2.1 Summary of data collection

This site was located between km 102 and km 103. It was investigated using 4 ERT survey lines (Figure 5.9). At this location, the road has a broad bend turning to the left. Because of this configuration, it was not possible to make long surveys parallel to the embankment. Thus, the 4 ERT surveys have different orientation to be able to encompass the entirety of the site. Survey 1 (S1) is located in the field, on the LHS. It is at the midpoint of the bend, with its ends being few meters away from the road. This area is located between the thaw lake on its west side, and the road on the east side. Some ice wedge polygons are present but hardly visible on the aerial imagery, nevertheless their surficial expression can be observed close to lake, where the flooded troughs are apparent. Survey 2 (S2) is located on the shoulder of the embankment, on the RHS of the road. The midpoint of this survey was immediately across from the rest area. Survey 3 (S3) is located in the field, on the RHS, at approximately the same level as S2. It is on a plateau about 2m higher in elevation than the road embankment. At S3, there is also polygonal ground that is hard to discern in aerial imagery but evident on the site where there is subtle surficial expression. Finally, survey 4 (S4) was located on the RHS along the embankment in the area where the lake is touching the road. This area is reportedly the most affected by subsidence.

At this site, the light portable drill was used to perform shallow drilling. Three shallow boreholes (DH103 BH1, 2, and 3) were drilled along S1, and a deeper borehole (DH102 BH1) was drilled along S3. The latter borehole was fitted with PVC piping and instrumented with 4-channel Hobo logger. Frozen cores were brought back to the NCE lab and analyzed for cryostratigraphic description, excess ground ice content, and grain size distribution.

At the time of the survey, no damage was observed on the road, on its shoulders, or at the toe of the embankment. However, the road was re-leveled few weeks after the survey.

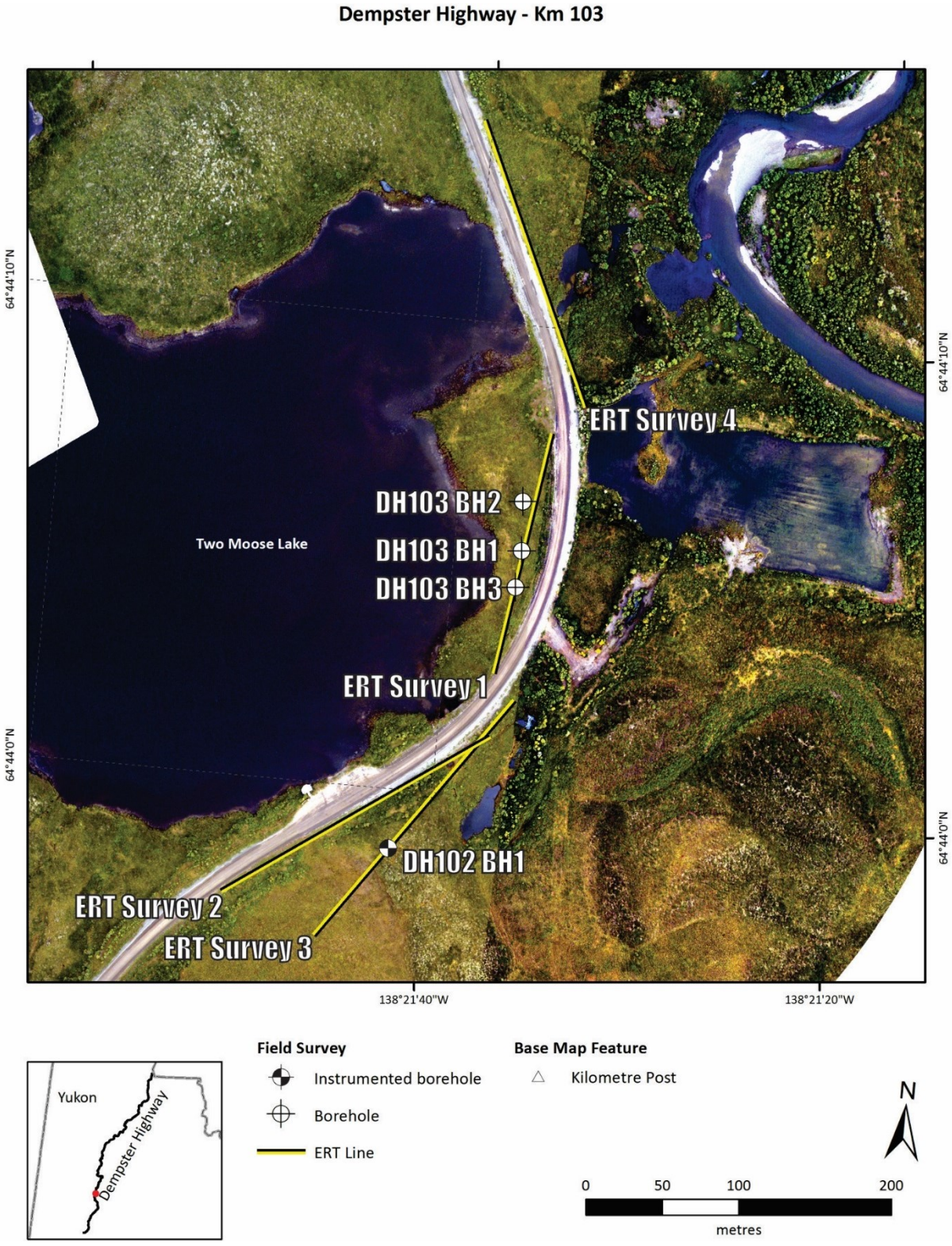

Figure 5.9. Survey site at km 102/103 with location of the ERT surveys, Boreholes, and noticeable features.

5.2.2 Borehole data

Logs

The boreholes made along the ERT survey 1 (S1) were all very shallow, not much more than 1 m depth. DH103 BH1 was drilled close to electrode 41, chaining 80 m from the first electrode located at the southern end of the survey. The thaw front at the borehole site was located at 39 cm depth and the stratigraphy consisted of organics from 0 to 18 cm, organic-rich silt from 18 to 30 cm, grey clayey silt from 30 to 71 cm, silty sand from 71 to 99 cm, and finally gravel, from 99 to 114 cm; the final depth of the borehole. DH103 BH2 was drilled near electrode 59 (chaining 116 m) on a small elevated mound, but reached gravel at only 50 cm, without reaching the thaw front. Finally, DH103 BH3 was performed at electrode 29 (56 m chaining). The thaw front was located at 30 cm and the stratigraphy consisted of organics from 0 to 20 cm, brown silty sand from 20 to 47 cm, medium to coarse sand from 47 to 64 cm, and coarse sand to gravel from 64 to 76 cm; the end of the drilling. All holes reached a gravel layer that prevented further drilling at the location of this survey. The gravel was rounded and appeared to be of fluvial origin which was consistent with the surficial geology map (Figure 2.2). The thaw depths at the time of the survey (July 27th) ranged from 30 cm in the field to 82 cm near to the road.

Borehole DH102-BH1 was drilled along ERT survey 3 (S3) near electrode 15, at chaining 70 m of the survey (Electrode 1 located at southern end), in middle of an ice wedge polygon. The thaw front was at 44 cm depth. The soil stratigraphy consisted of moss and peat from 0 to 20 cm, organic rich silty sand from 20 to 75 cm, and then a sediment alternating between silty sand and sandy silt down to about 290 cm. The lower part of the profile had a layer of sand from 290 cm until termination on a gravel layer at 316 cm. Excess ice contents range from 12 to 63%, the lowest contents being in the lower part of the profile.

Ground temperature

Borehole DH102-BH1 was lined with PVC piping and instrumented with a 4-channel Hobo logger to record ground temperatures at 0, 0.5, 1.5, and 3.16 m depths. The recording started July 30th, 2016, at 16H00. No data have been downloaded at the time. Ground temperature data from this site will be retrieved in June 2017, and added as an addendum to this report when available.

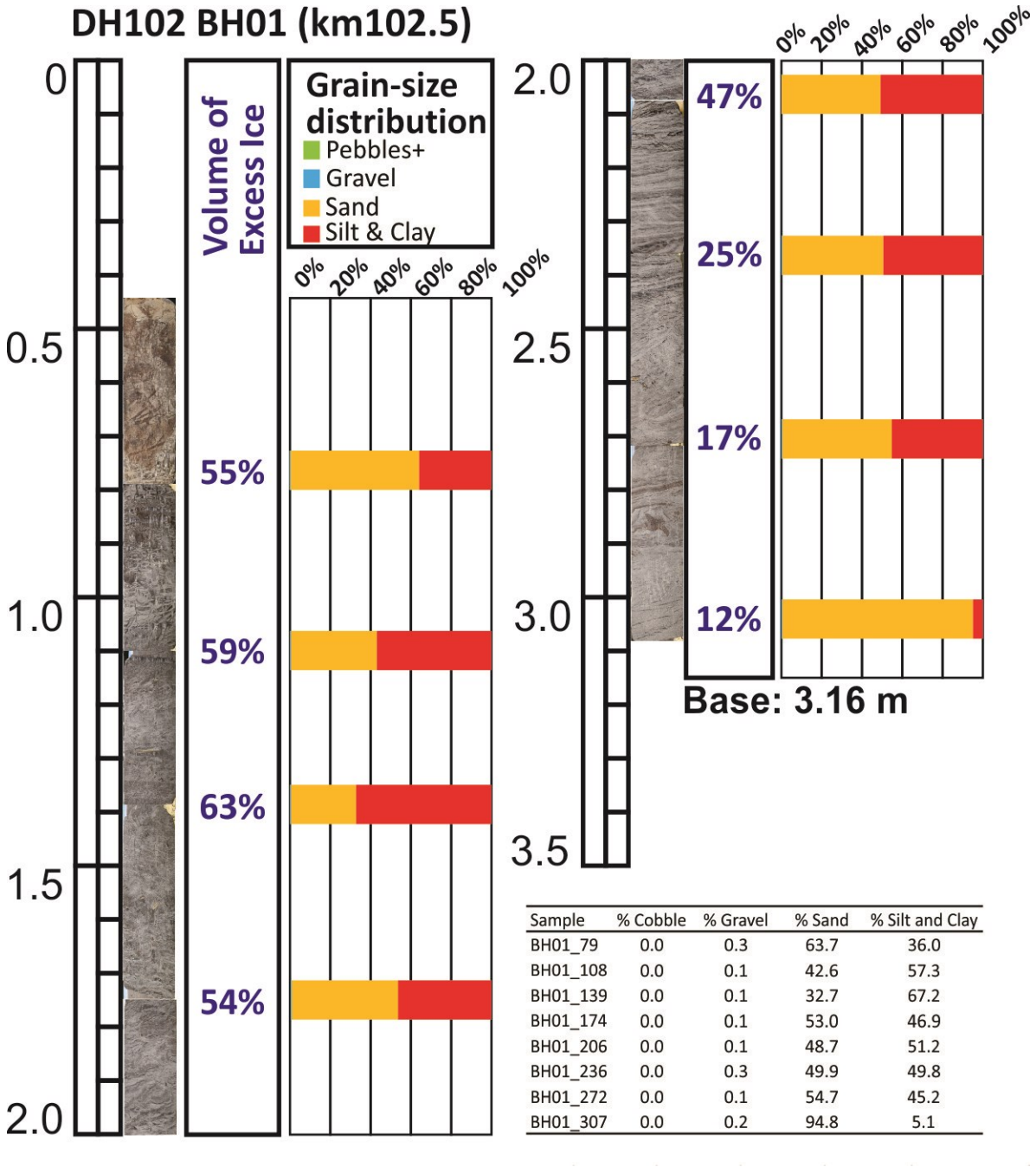

Sample	% Cobble	% Gravel	% Sand	% Silt and Clay
BH01_79	0.0	0.3	63.7	36.0
BH01_108	0.0	0.1	42.6	57.3
BH01_139	0.0	0.1	32.7	67.2
BH01_174	0.0	0.1	53.0	46.9
BH01_206	0.0	0.1	48.7	51.2
BH01_236	0.0	0.3	49.9	49.8
BH01_272	0.0	0.1	54.7	45.2
BH01_307	0.0	0.2	94.8	5.1

Figure 5.10. Borehole log, excess ice content, and grain size analyses for DH102-BH1.

5.2.3 ERT surveys

The ERT surveys are presented in Figures 5.11, 5.12, and 5.13. They are not presented in the order of their acquisition, but from the South at the top to the North at the bottom (S2, S3, S1, and S4). All the profiles were oriented South to North (i.e., electrode 1 at the South end, electrode 81 at the North end).

Survey 2 – RHS – Shoulder of the embankment

Wenner array - Survey 2 (Figure 5.11): The resistivity profile can be interpreted along either vertical or horizontal orientations. Vertically, there is an upper area showing lower resistivity values of the survey, ≤1000 ohm.m, that can be found down to 6 m depth, and a deeper area where the resistivity values can be tens of thousands ohm.m. Horizontally, the southern part of the profile shows the highest resistivity values in the shape of a high-resistivity block, while the northern part has generally smaller resistivity values, but with another very high resistivity area between about 130 and 170 m chaining. The south and north parts are separated by a vertical boundary located at approximately 100 m chaining. The blocky appearance of the profile may be because the electrical current cannot pass through the ground. In this area, the magnitude of the resistivity may be overestimated due to the inability of the current to pass to greater depth. Even with this in mind, the profile can be interpreted as showing massive ground ice at relatively shallow depth between chaining 0-100 m and 125-180 m approximately. While its vertical extent cannot be estimated at the southern portion of the survey, it does not extend deeper than 13 to 17 m in the northern section.

Dipole-dipole array - Survey 2 (Figure 5.12): The dipole-dipole resistivity profile shows the same type of resistivity distribution as the Wenner survey, but with a sharper image of the permafrost condition. In the southern section of the profile of the section, two high resistivity zones appear within a larger one; from chaining 16 to 38 m, and from chaining 50 to 106 m, approximately. In the northern section, a large resistivity area spreads from chaining 110 to 168 m, with a very high resistivity from chaining 124 to 148 m, approximately. A final smaller area of high resistivity is present between chaining 174 and 180 m, approximately. The high resistivity areas are between approximately 3 and 16 m depths. The presence of a culvert at 170 m chaining, may be contributing to lower resistivity either because of the influence of the metallic pipe, or because of the thermal effect of the culvert and the induced thaw, as a small pond is present here. At the depth of roughly 20 m, the resistivity values drop drastically. A plausible interpretation of this profile is that the high resistivity areas are bodies of massive ice, with maximum thickness that may range between 6 m and 10 m. The lower resistivity areas may be either bedrock or unfrozen ground.

Gradient array - Survey 2 (Figure 4.13): The resistivity profile obtained with the gradient survey is similar to the one obtained with the Wenner array. It displays the same vertical and horizontal characteristics. The vertical and horizontal boundaries between each high resistivity area are very similar. The only significant difference is the resistivity values that are much higher in the gradient survey, as resistivity values can exceed 100,000 ohm.m. This could be attributable to the difficulty of this specific array configuration to propagate electricity in this specific geological setting. The influence of the culvert at 170 m chaining is also visible.

Survey 3 – RHS – Field – 5 to 50 m away from the embankment

Wenner array - Survey 3 (Figure 5.11): The surface condition of the survey varies significantly along the profile. From chaining 0 to about 64 m, there is a low-elevation marshy area, then there is higher polygonal plateau until about chaining 100 m. Beyond this small plateau, a downhill slope leads to a lower marshy area and a small pond between chaining 135 and 140 m (the same as the one described in Survey 2) and finally a flat bushy area until its end. The ERT survey seems to partially reflect this surficial condition. The southern end of the section shows low resistivity values in the humid area, down to about 6 m depth; resistivity values are much higher below this depth. The resistivity values are high from the surface down over the dry polygonal ground. The first 4 m of the profile may reflect the presence of the frozen ice-rich fine sediment. This is consistent with the observation made from borehole DH102-BH1. Below this depth, the resistivity increases considerably down to approximately 16 m depth. This could be attributed to frozen gravel or the presence of massive ice. Further north along the survey, the resistivity generally decreases, the lowest values being recorded at the level of the water ponding. Overall, below 16 m depth, the resistivity value decreases progressively but remains relatively high (between 5,000+ and 2,000 ohm.m). This could be attributable to coarse sediment, bedrock, or the influence of the overlying very resistive layer. Considering the geomorphological context and the subsidence occurring in the whole area, it can be assumed that the very high resistivity zones are massive ice.

Dipole-dipole array - Survey 3 (Figure 5.12): Survey S3 was similar to S2 in that the dipole-dipole array appears to be better defined than the Wenner array. In general, the pattern of the resistivity is very similar, with the dipole-dipole array resistivity values slightly higher than the Wenner array. However, two significant differences can be reported. First, the area of high resistivity below the polygonal ground spreads further north that what was detected using the Wenner survey (as far as chaining 125 m). The very high resistive core of this area detected between 4 m and 12 m depths. In addition, between 0 and 4 m depths, there is a pattern of lower and higher resistivity values along the chaining. It is probable that the higher resistive values represent ice-wedges. The second difference is that there is a low resistivity area located between 100 m and 130 m chaining, at depths ranging between 12 m and 20 m, approximately.

To the North, lower resistivity values continue in the deeper part of the profile. Laterally, this low resistivity zone coincides with the presence of a sequence of ponds located about 25 m east of the survey. It can be hypothesized that the low resistivity area between 100-130 m is an unfrozen area where subsurface water from Two Moose Lake connects with the biggest pond in the field.

Gradient array - Survey 3 (Figure 5.13): The gradient array shows results that are very similar to the dipole-dipole survey, but with less defined features. The characteristics of the high resistivity areas located under the polygonal ground plateau are mainly the same, but the lower resistivity area below chaining 100-120 m is more diffuse in nature. The low resistivity area starting at about chaining 155 m, already described in the Wenner array, seems to be enhanced in the gradient array, starting at about 5 m depth. At this location, the gradient array does not provide additional information.

Survey 1 – LHS – Field – 5 to 25 m away from the embankment

Wenner array - Survey 1 (Figure 5.11): The ERT profile show mostly higher resistivity values in the upper part of the profile and lower ones deeper down. Three areas show resistivity values ranging from 6,000 to 10,000+ ohm.m, at chaining 20-40 m, 65-90 m, and 100-125 m approximately. These areas occur between 2 and 6 m depths, approximately, and could coincide with ice-wedge polygons. The surrounding ground could also be ice-rich as the resistivity values are above 2,000 ohm.m. There is a horizontal 2000 ohm.m boundary at about 8 m depth. This boundary underlies almost the entire profile; it clearly separates shallow resistive ground from deeper low-resistivity ground. The Northern section of the profile, past chaining 60 m, has resistivity values that are lower than 400 ohm.m. The area might be unfrozen, and even wet because this part of the survey is located between Two Moose Lake to the west and an artificial, excavated lake, to the east. The presence of nearby water bodies may contribute to lower resistivity values by warming permafrost either by infiltration of ground water or by thermal influence.

Dipole-dipole array - Survey 1 (Figure 4.12): Adding to the results from the Wenner array, the dipole dipole array results indicate that there are high resistivity areas at both southern and northern ends of the survey. These observations should be considered with caution because these areas are located at the edge of the profile and it could be an artefact of the inversion process. The dipole-dipole array results also show another low resistivity area located between chaining 50 and 60 m, between 6 and 26 m depths, approximately. At this location, the lake is only just over 10 m west of the survey. Finally, the large, low-resistivity area located north of chaining 70 m has better defined lower boundaries than the Wenner survey. Resistivity values appear to slightly increase below 20 m depth, between chaining 66 and 96 m, approximately.

High-resistive zones still are present all along the length of the profile between 1 and 6 m depths, that may represent massive ice, either buried or ice-wedge.

Gradient array - Survey 1 (Figure 4.13): the gradient array shows a compromise between the two previous arrays. It shows a horizontal boundary between high and low resistivity areas at approximately 6 m depth with slightly higher resistivity between chaining 20 and 50 m below this depth. A high resistivity area is present below 20 m depth at chaining 50 m, as already described for the gradient array. It is important to note than the Wenner and gradient profile are shallower and also have steeper slope on their boundaries. For example, at 24 m depth, these arrays provide information only between chaining 64-96 m and chaining 52-108 m for the Wenner and Gradient arrays, respectively, while the dipole-dipole survey covers 30 to130 m chaining for the same depth.

Survey 4 – RHS – Shoulder of the embankment

Wenner array - Survey 4 (Figure 5.11): The major feature of this ERT profile is a large low resistivity area spreading from chaining 40 m to 130 m, and from the top of the profile to the bottom. Only one high resistivity area appears in this section of the profile between chaining 100 to 130 m, from 2 to 7 m depths approximately. Each end of the profile shows higher resistivity areas, from 10 to 40 m chaining at the south, and from 130 m to the end of the survey at the north. In the northern end, resistivity values increase to over 9,000 ohm.m, suggesting the presence of massive ground ice or very ice-rich permafrost. The very low resistivity values observed between chaining 40-130 m suggest that it is possible that some groundwater may pass under the embankment.

Dipole-dipole array - Survey 4 (Figure 5.12): Because the dipole-dipole array provides a deeper and wider window of investigation than the Wenner array, it better shows the high resistivity area in the southern end that was not apparent in the Wenner survey. The resistivity values are over 10,000 ohm.m and suggest the presence of massive ice. North of this, values decrease drastically, even in the deepest part of the profile, with resistivity values <200 ohm.m. Within this relatively low resistivity environment, three high-resistivity areas are present: one between chaining 95-108 m from 4 to 12 m depths, another between chaining 132-154 m from 4 to 25 m depths, and a last one between chaining 165 m to the end of the survey, from 4 to 20+ m depths. The two last areas may also be attributable to the presence of massive ice.

Gradient array - Survey 4 (Figure 5.13): Once again, the gradient survey shows a compromise between the Wenner and dipole-dipole arrays, and underscore the very low resistivity values present in the southern half of the profile. A relatively small restive area is present at shallow depths between 10 and 20 m chaining, that was not detected using the two previous arrays. There is no clear explanation for this singular feature.

5.2.4 Interpretation

The ERT surveys at km 102-103 indicate 3 possible features: 1- Ice-rich permafrost; 2- massive ground ice bodies - either ice-wedges or buried ice; and 3- possible ground water movement. Figure 5.14 shows the plan view of the site with the plausible locations of these features as suggested by merging the observations from the three ERT arrays.

The ice rich permafrost and massive ground ice bodies may be responsible for the general subsidence observed on this section on the road. Ground water movement may also be influencing ground movement in the northern part of the study area. This is the location where the lake is at the west foot of the road embankment.

In this area, the northern-most section may be partly underlain ice-rich permafrost and massive ice that may contribute to subsidence when they thaw. In the southern part of ERT S4, permafrost is absent, and underground water seeping from the lake to the river nearby may be responsible for leaching sediment and contributing to the subsidence.

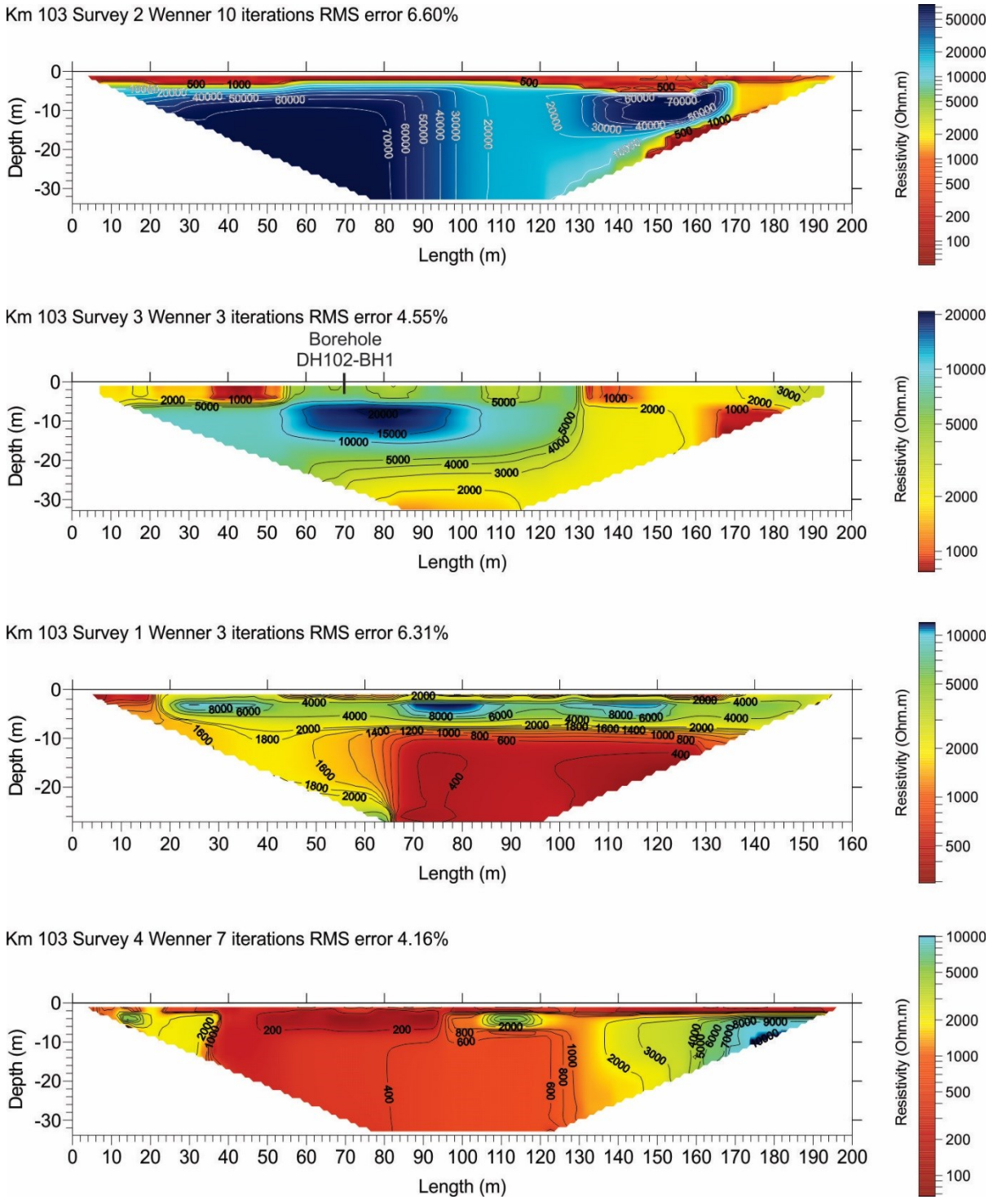

Figure 5.11. Surveys 1-4 using Wenner array at km 102-103 sites

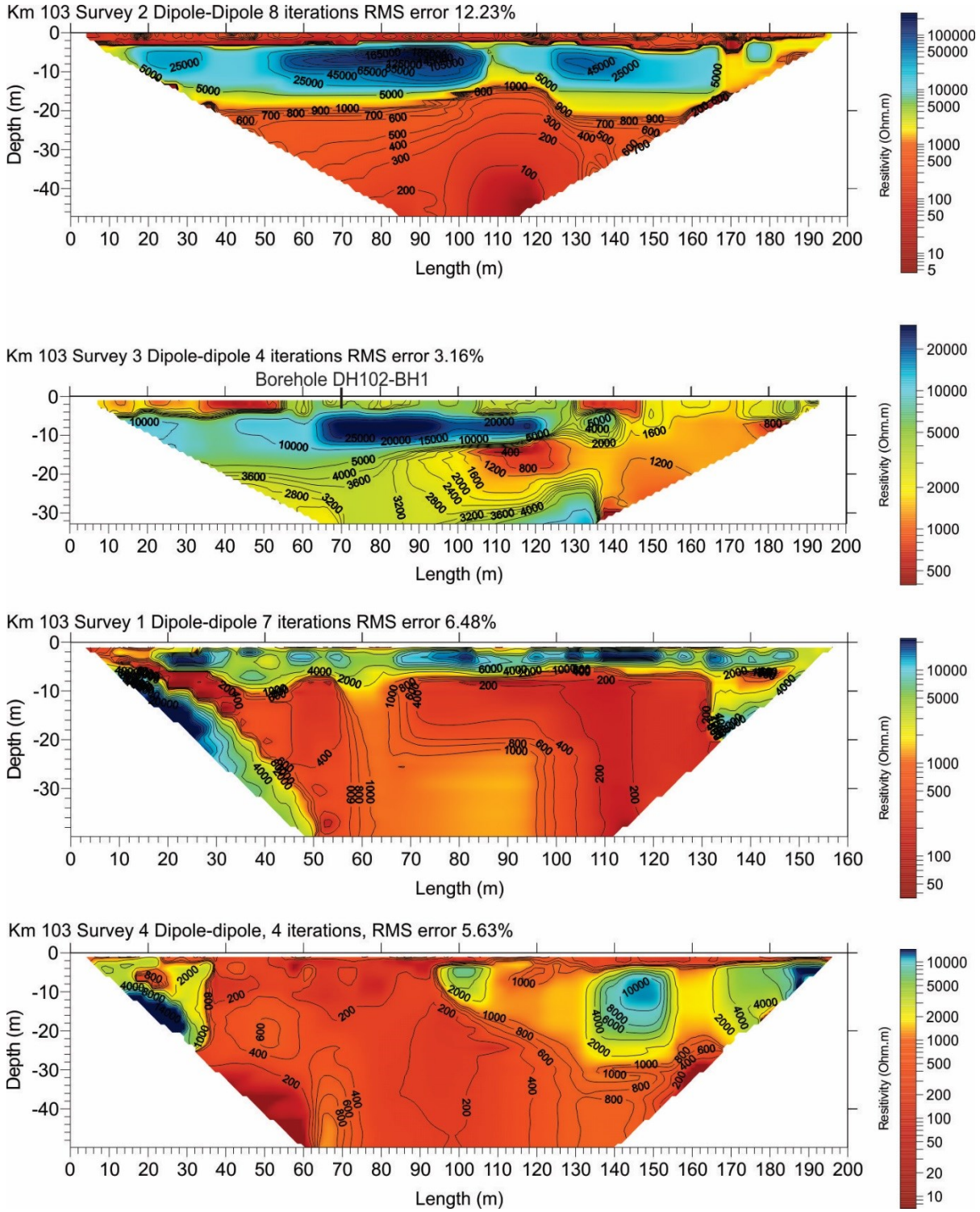

Figure 5.12. Surveys 1-4 using dipole-dipole array at km 102-103 sites.

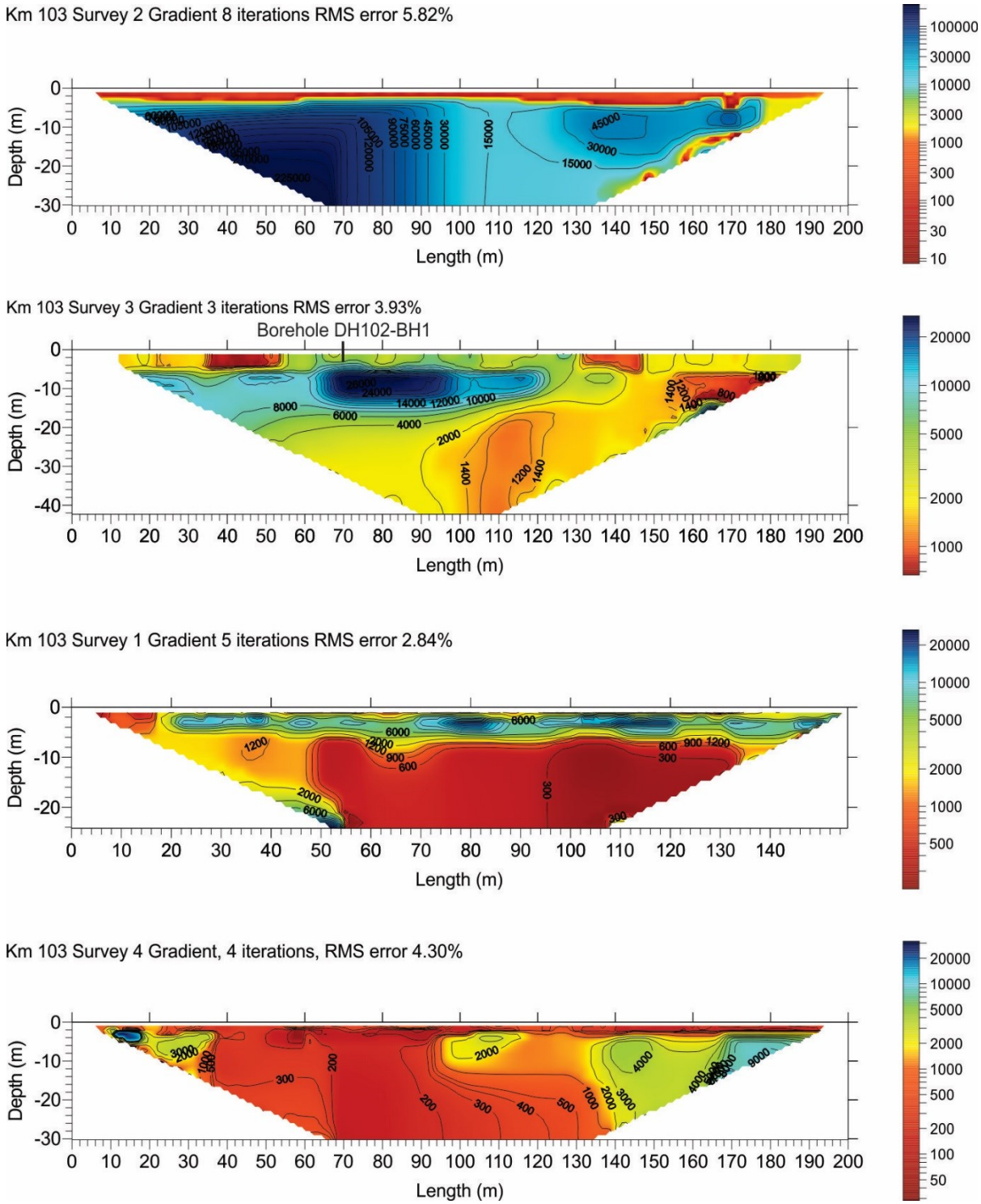

Figure 5.13. Surveys 1-4 using gradient array at km 102-103 sites.

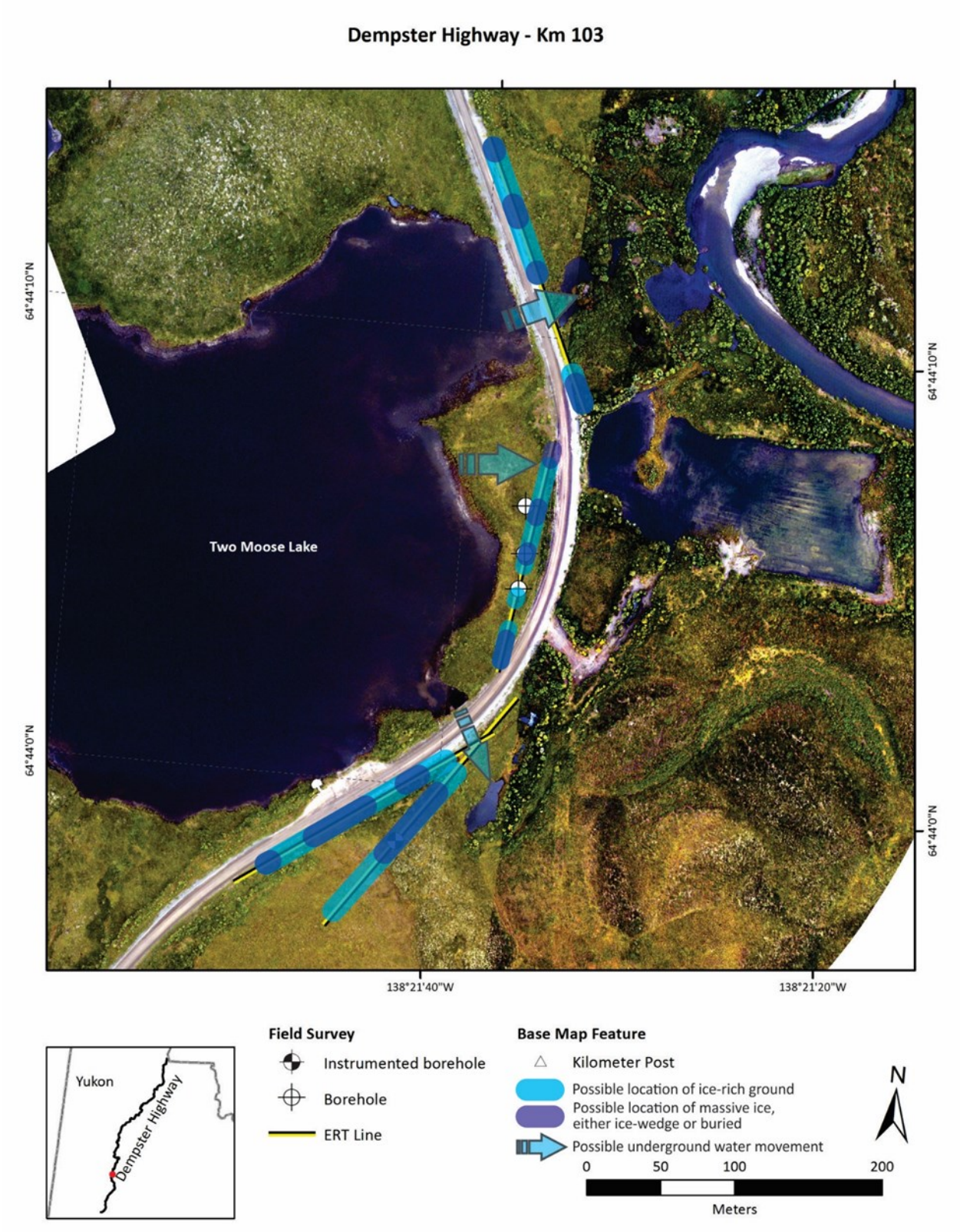

Figure 5.14. Site view with features inferred from the ERT surveys.

6. CONCLUSION

Two main hypotheses were investigated to explain sinkhole formation and subsidence at each site. The first hypothesis is that the thaw of ice-rich permafrost or/and massive ice bodies is resulting in a loss of volume that contributes to subsidence and caving. The second hypothesis is that recession of permafrost is opening new pathways for ground water to leach fine-grained material leading to the creation of void spaces where there was previously frozen sediment.

Based on our analyses, borehole data provide no evidence of ice-rich ground or massive ice at km 82. Rapid spikes in ground temperature following precipitation events are an indication of movement of ground water and high hydraulic permeability of sediments. ERT surveys show some variation in resistivity that could be attributable to changes ground ice content, soil texture, and/or wetness. The resistivity values remain relatively low, which does not support the hypothesis that massive ice is contributing to sinkhole formation. In addition, the survey led by GroundTruth Exploration suggests a relationship between topography, surface water movement and sinkhole location. Details of this relationship were not explored further. Based on the available information, there is more evidence to support the hypothesis that groundwater movement and leaching are responsible for sinkhole formation than evidence to support that issues are related to massive ice at km 82. A deeper investigation may also determine whether channeling of surface water by topography and subsequent infiltration and leaching are also contributing. With the current understanding of the issues at km 82, three remedial actions are suggested for HPW consideration:

- Prevent snow accumulation: The depressed area on the RHS of the road between the road embankment and a cut in the slope should be kept free of snow. This snow insulates ground in winter and introduces water when it melts in spring, thereby contributing to permafrost degradation. Snow could be cleared; or the depressed area could be filled and levelled to prevent snow accumulation and promote permafrost aggradation.
- Ensure the culvert is opened at the time of freshet: During a visit to the site, it was observed that the culvert was plugged with ice at the time of the freshet. This may promote water accumulation or the flow of the runoff along the foot of the embankment rather than through the culverts.
- Prevention water infiltration nearby the road: Options could be studied such as the use of an impervious geotextile to prevent infiltration close to the road, and/or lining and excavation of the ditch to ensure runoff to conveyed through the culverts. The replacement of the culvert at this site in Fall 2015 may have achieved this objective already, but it is too soon to know the impact of this work on permafrost.

For km102-103, our assessment is mostly based on the ERT surveys and field observations. Shallow boreholes drilled by hand provided information about near-surface characteristics, but drilling of a geotechnical borehole would likely provide critical information. The geomorphological survey suggests that the geology of the site consists of a fluvial or glaciofluvial gravel covered by a fine-grained sediment veneer. Ice-wedge polygonal ground has developed in the upper layer. Though not confirmed at km 102-103, observations from km 124 suggest that the ice-wedges may be restricted to this thin upper layer. Direct observations in the face of a rotational slump at km 117 show the presence of massive ice, probably from glacial origin, buried within the gravel. In the absence of any other major surficial characteristics, it is reasonable to conclude that both the thin ice-wedges and buried ice in the underlying gravel are present at the km 102-103 site. The ERT surveys show very high resistivity areas that likely correspond with the presence of massive ice bodies, either ice wedge or buried ice. The thaw of this massive ice may be responsible for some of the subsidence at the site. However, at the location where the lake is washing the LHS foot of the road and there has been extensive subsidence, there is no evidence of permafrost. Just north of this location, there is potentially ice-rich permafrost. The permafrost-free location may constitute a spillway to the nearby Blackstone River. Consequently, there is evidence to support both the massive ice and leaching hypotheses at this site. The two processes could continue at this location as permafrost retreats. While the ground ice can melt at the north end of S4, groundwater flow may leach out sediment at the south end.

Considering the nature of the issues at km 102-103, possible actions included the following:

- Ground truthing using geotechnical boreholes at specific locations. ERT results indicate a number of locations where wedge and massive ice are suspected. Geotechnical boreholes (at least 20m) would confirm or refute these geophysical observations, and establish the vertical extent of ground ice and the depth of bedrock.
- If leaching is confirmed as a contributor to subsidence, excavation could be performed to remove fine-grained material below embankment, and replace it with rocky and boulder material with a low-fine content matrix.

REFERENCES

Andersland, O.B., Ladanyi, B. 2004. Frozen Ground Engineering. 2nd Edition. John Wiley & Sons, 384 p.

Beirle, B.D., 2002. Late Quaternary glaciation in the Northern Ogilvie Mountains: revised correlations and implications for the stratigraphic record. Canadian Journal of Earth Sciences 39, 1709–1717.

Bostock, H.S., 1966. Notes on glaciation in central Yukon Territory. Geological Survey of Canada Paper 65-36.

Burn, C.R., 1994. Permafrost, tectonics and past and future regional climate change, Yukon and adjacent Northwest Territories. Canadian Journal of Earth Sciences 31, 182–191.

Burn, C., Moore, J., O'Neil, B., Hayley, D., Trimble, R., Calmels, F., Orban, S., and Idrees, M. 2015. Permafrost characterization of the Dempster Highway, Yukon and Northwest Territories. GEOQuébec2014: 64th Canadian Geotechnical Conference & 7th Canadian Permafrost Conference, Sept. 20-23, 2015, Québec, Québec. Canadian Geotechnical Society.

Calmels, F., Gagnon, O.; and Allard, M. 2005. A portable earth-drill system for permafrost studies. Permafrost and Periglacial Processes 16: 311-315.

DMT Geoscience Ltd. 2015. Geophysical Investigation, Various Locations, Campbell Highway #4: KM34-35; Dempster Highway #5: KM34-36, KM71-130. 51 p.

Froese, D.G., and Zazula, G.D. 2003. Field guide to quaternary research in the klondike goldfields. Third International Mammoth Conference, Occasional Papers in Earth Sciences No. 6. http://www.tc.gov.yk.ca/publications/IMC_Field_Guide_2003.pdf

GroundTruth Exploration. 2015. Sinkhole Detection & Assesment Using High Resolution DC Resistivity & UAV Drone Imagery. 25 p.

Environment Canada, 2004. Canadian Climate Normals 1971–2001. Canada Atmospheric Environment Service, Minister of Supply and Services Canada, Ottawa, ON, Canada.

French, H., and Shur, Y. 2010. The principles of cryostratigraphy, Earth-Science Reviews, 101: 190-206.

Green, L.H., 1972. Geology of Nash Creek, Larsen Creek, and Dawson map areas. Geological Survey of Canada, Memoir 364, 157 p.

Heginbottom, J.A., Dubreil, M.A., Harker, P.T., 1995. Canada Permafrost Map, 1:5,000,000, scale. National Atlas of Canada, 5th edition, Government of Canada, Ottawa.

Idrees, M., Burn, C., Moore, J., and Calmels, F. 2015. Monitoring permafrost conditions along the Dempster Highway. GEOQuébec2014: 64th Canadian Geotechnical Conference & 7th Canadian Permafrost Conference, Sept. 20-23, 2015, Québec, Québec. Canadian Geotechnical Society.

Lacelle, D., Lauriol, B., Clark, I. D., Cardyn, R., & Zdanowicz, C. (2007). Nature and origin of a Pleistocene-age massive ground-ice body exposed in the Chapman Lake moraine complex, central Yukon Territory, Canada. Quaternary Research, 68(2), 249-260

SRK Consulting (Canada) Inc. 2014. Desktop Study – Sinkhole Site Characterization. Demspter Highway, Yukon Territory. 27 p.